DESIGN OF DIGITAL BAND PASS FILTER AND ITS APPLICATION TO RANDOM WATER WAVE DATA

by
K. S. Su
and
Erich J. Plate

March 1969

CER68-69KSS25

ABSTRACT

In this report the design of a digital band pass filter is discussed. It consists of an approximation to the ideal rectangular frequency filter. The data are convoluted with a truncated Sinc function. Theoretically, the Fourier transform (Frequency response) of the Sinc function is the ideal low pass filter in the frequency domain. The difference of two such low pass filters of different cut-off frequencies gives a band pass filter with a suitably chosen narrow bandwidth. A band pass filter consisting of a truncated Sinc function does not have ideal shape, but by keeping the truncation limits 6 to 8 times wider than the main lobe of the Sinc function, this filter has a sharper cut-off than that used by Blackman-Tukey.

The filter is applied to the determination of properties of particular frequency components of wind water waves. These components are filtered from the original record of water surface displacement with the aid of a digital computer. In this manner the statistical properties of the water surface, which include wave spectra, auto-correlation, and space-time correlation were studied.

The variance calculated from a filtered time series of particular frequency component represents the wave energy at that filtered

frequency band. Spectra constructed by this technique are in good agreement with those obtained by the Blackman-Tukey method. Filtered space-time correlations showed that the propagation speed of a water wave is independent of frequency component, and is governed by the dominant frequency of original time series only.

ACKNOWLEDGMENTS

The author wishes to express his sincere appreciation to his major professor, Dr. E. J. Plate, for his guidance, continuous encouragement and inspiration during the course of his study and writing of his thesis.

For their comments and review of the thesis, gratitude is extended to Professors R. N. Meroney and R. J. Morgan.

Credit is also due Drs. S. Karaki and J. Gessler for their constant assistance and suggestions.

Mr. Ralph V. Asmus, shop foreman, and other personnel of the hydraulics laboratory materially assisted with the development of experimental equipment.

Special appreciation also goes to those who assisted in reducing the data, drafting, typing and printing of this thesis: Mr. Y. H. Cheng, Miss Hanae Akari, Mrs. Pat Tagader, Mrs. Arlene Nelson, and Mrs. Mary Fox.

TABLE OF CONTENTS

LIST OF TABLES

LIST OF FIGURES

LIST OF SYMBOLS

Symbols	Definition
A	Fourier transformed function
C	Wave propagation speed (m/sec)
d	Water depth in wind-water tunnel
f	Frequency in Hz
f_c	Central frequency
g	Gravitational acceleration
K	Wave number
m	Mean of random time function
n	Scale factor
R	Correlation coefficient
R(f)	Frequency response function
S	Energy spectrum
T	Height of equally weighted function
T_o	Length of rectangular function
T_s	Length of main lobe of Sinc function
t	Time
w(t)	Weight function
x	Smoothed random time function
y	Stationary random time series
α	Ratio of length of Sinc function to the length of main lobe of that function

LIST OF SYMBOLS - CONTINUED

Symbols

β	Bandwidth, in terms of filtered central frequency
w	Angular frequency defined as $2\pi f$
τ	Time delay (second)
ψ	Space-time correlation function
σ	Standard deviation
δ	Distance between two probes

Any other symbols which do not appear here will be described whenever they first appear in the text.

Chapter I

INTRODUCTION

1.1 Purpose

When wind blows over the surface of moving or standing water, waves will be generated. These waves have different properties at different fetches or wind velocities. Part of these properties, such as the energy spectrum, and the basic propagation speed of the waves can easily be obtained from the original wave record by calculating , respectively, the variance spectrum of the record and the cross-correlation between simultaneous records taken at stations a short distance apart. These techniques do not permit inferring all the properties of the random water wave data associated with a particular frequency component. The wave record is mostly characterized by the wave components near the peak of the energy spectrum. However, frequency components associated with the first and second harmonic of the frequency of the peak also play a very important role in describing the wave shape.

For studying them, it is necessary to isolate a time series associated with a particular frequency component from the given original time series. In the time domain, if we introduce a weight function $W(t)$ and apply it to the original wave record $y_1(t)$ a weighted running mean or convolution is obtained:

$$\hat{X}_i(\omega_i, t_j) = \int_{-\infty}^{\infty} y_i(t)\, w(t_j - t)\, dt \quad . \tag{1-1}$$

The Fourier transform of Eq. 1-1 is found, by the convolution theorem of Fourier integral theory to:

$$A_x(\omega_i) = \left[A_x(\omega) \right] \text{F.T.}\left(w_i(t) \right) \quad , \tag{1-2}$$

For this study, a weight function $w_1(t)$ is chosen which yields a low pass filter, with a cut-off frequency of ω_1, say , repeating the filtering with a different cut-off frequency ω_2, and taking the difference of the two filtered functions, then a band pass filtered time series $x(\omega, t)$ is obtained:

$$X(\omega, t) = \hat{X}_1(\omega_1, t) - \hat{X}_2(\omega_2, t) \quad . \tag{1-3}$$

where amplitude spectral density is given to

$$A_x(\omega_2 \sim \omega_1) = A_x(\omega) \left[\text{F.T.} \left| w_1(t) - w_2(t) \right| \right] \quad , \tag{1-4}$$

where the term in $\{\}$ yields a band pass filter with center frequency $(\omega_1 + \omega_2)/2$ and band width about $\omega_2 - \omega_1$.

An ideal band pass filter which passes only the frequency components within the band requires a weight function which extends from $-\infty < t < \infty$. Consequently, some compromise has to be made.

In this thesis, most of the effort is directed towards designing a filter whose properties resemble those of the ideal filter. The weight function chosen is the truncated sinc-function, and a major problem was to obtain its Fourier transform.

1.2 Literature Review

Holloway (1958) combined most of the pertinent information of filtering and smoothing into a concise, simple form. He discussed different filters. The frequency response function of a filter is defined as the transform function R(f) of a given weight function $\omega(t)$ with which the data record is convoluted. It is given as:

$$R(f) = Re\left[\int_{-\infty}^{\infty} \omega(t) \exp(2\pi i f t)\, dt\right]$$

$$= \int_{-\infty}^{\infty} \omega(t) \cos(2\pi f t)\, dt \quad , \qquad (1\text{-}5)$$

where R(f) is frequency response function, and ω (t) is weight function.

Holloway discussed the theoretical frequency response of the following low pass filters:

(a) The equal weight filter which is defined by:

$$w(t) = \begin{cases} \frac{1}{T} & , \ |t| \leq \frac{T}{2} \\ 0 & , \ |t| > \frac{T}{2} \end{cases}$$

where $1/T$ is the height of the weight function.

(b) The filter defined by the normal probability curve:

$$w(t) = (2\pi\sigma^2)^{-\frac{1}{2}} \exp(-t^2/2\sigma^2)$$

where a is the standard deviation, and

(c) The filter given by the exponential function:

$$w(t) = \begin{cases} 0 & , \ t < 0 \\ (\lambda^{-1}) \exp(t/\lambda) & , \ t \leq 0 \end{cases}$$

where λ is the lag coefficient.

The frequency response curves of (a), (b), and (c) are shown in Fig. 1. Unfortunately, none of these curves is ideal, because they do not give a sharp cutoff frequency. (Usually, the cutoff frequency is taken as the frequency where the response drops to 1 or 2 percent.) Furthermore, large side lobes of the filter cause a leakage into bands beyond the cutoff frequency. If a band pass filter is constructed from these stated weight functions, its shape is even less satisfactory than that of low pass filters. Theoretically, the ideal low pass filter must be a rectangular window:

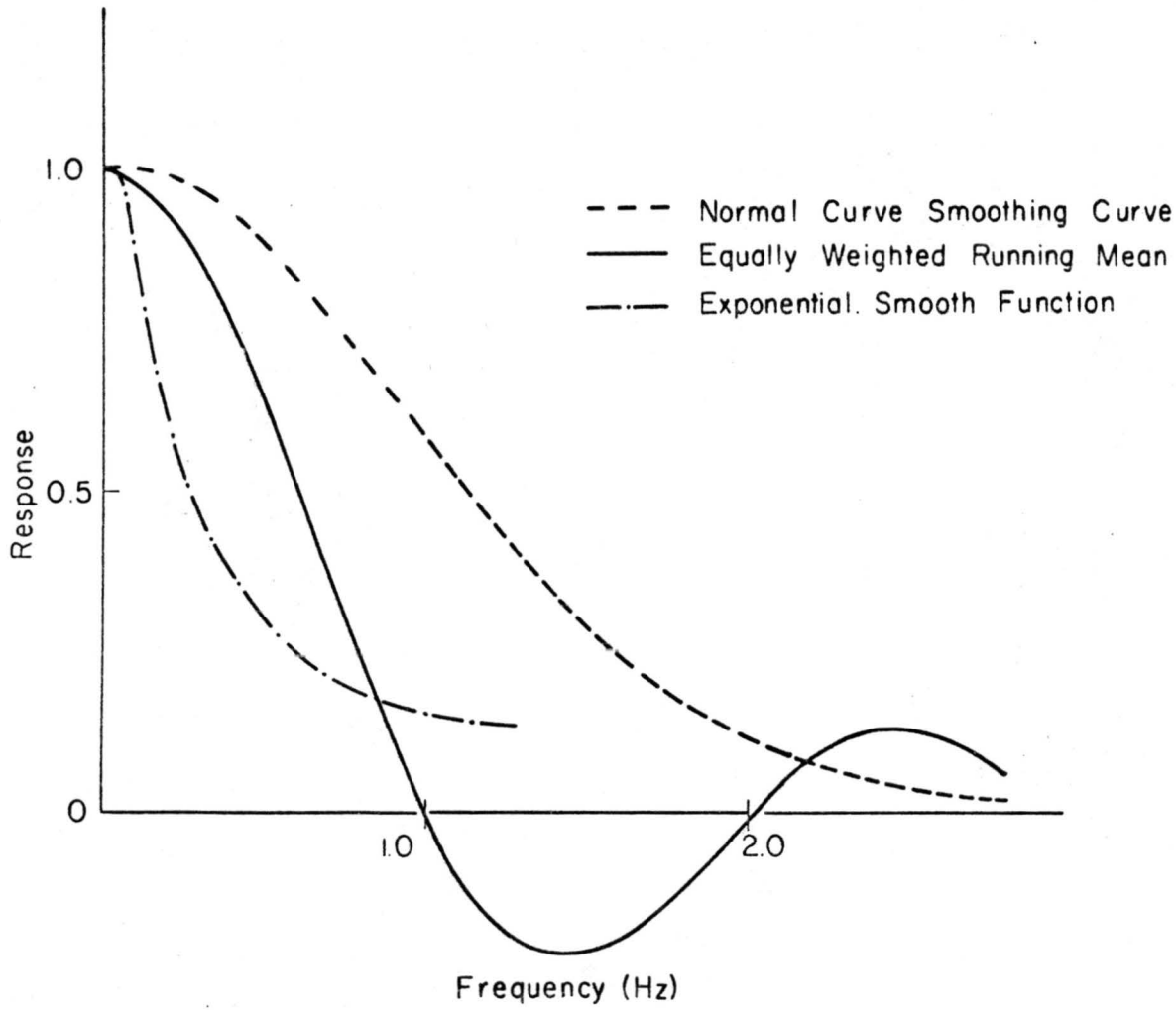

Fig. 1. Comparison of frequency response curves of equal weight, normal probability, and exponential curves.

$$R(f) = \begin{cases} 1 & , \quad 0 \leq f \leq f_c \\ 0 & , \quad f > f_c \end{cases}$$

Unfortunately, the corresponding weight (filter) function is:

$$\begin{aligned} W(t) &= \int_{-\infty}^{\infty} R(f) \exp(2\pi i f t)\, df \\ &= 2\int_{0}^{f_c} \cos(2\pi f t)\, df \\ &= \frac{\sin(2\pi f_c)t}{\pi t (2f_c)} \quad (2f_c) \\ &= 2f_c \sin(2f_c t) \quad , \end{aligned} \tag{1-6}$$

which extends from $-\infty$ to $+\infty$. In discussing this weight function, Holloway states: "This smoothing function is a damped wave extending forward and backward in time from the origin. However, because the damping is rather slow, this function will often be impractical to use, since it will extend over so much of the series to be smoothed. The function can, of course, be taken to be zero (truncated) at some convenient distance on each side of the origin, but this alters the response in an undesirable way, and the closer to the origin it is truncated, the less desirable the response becomes." Figure 2 shows the comparison of frequency response of Sinc, truncated Sinc (truncated beyond the first negative lobes on either side of central positive lobe), and normal curve smoothing function.

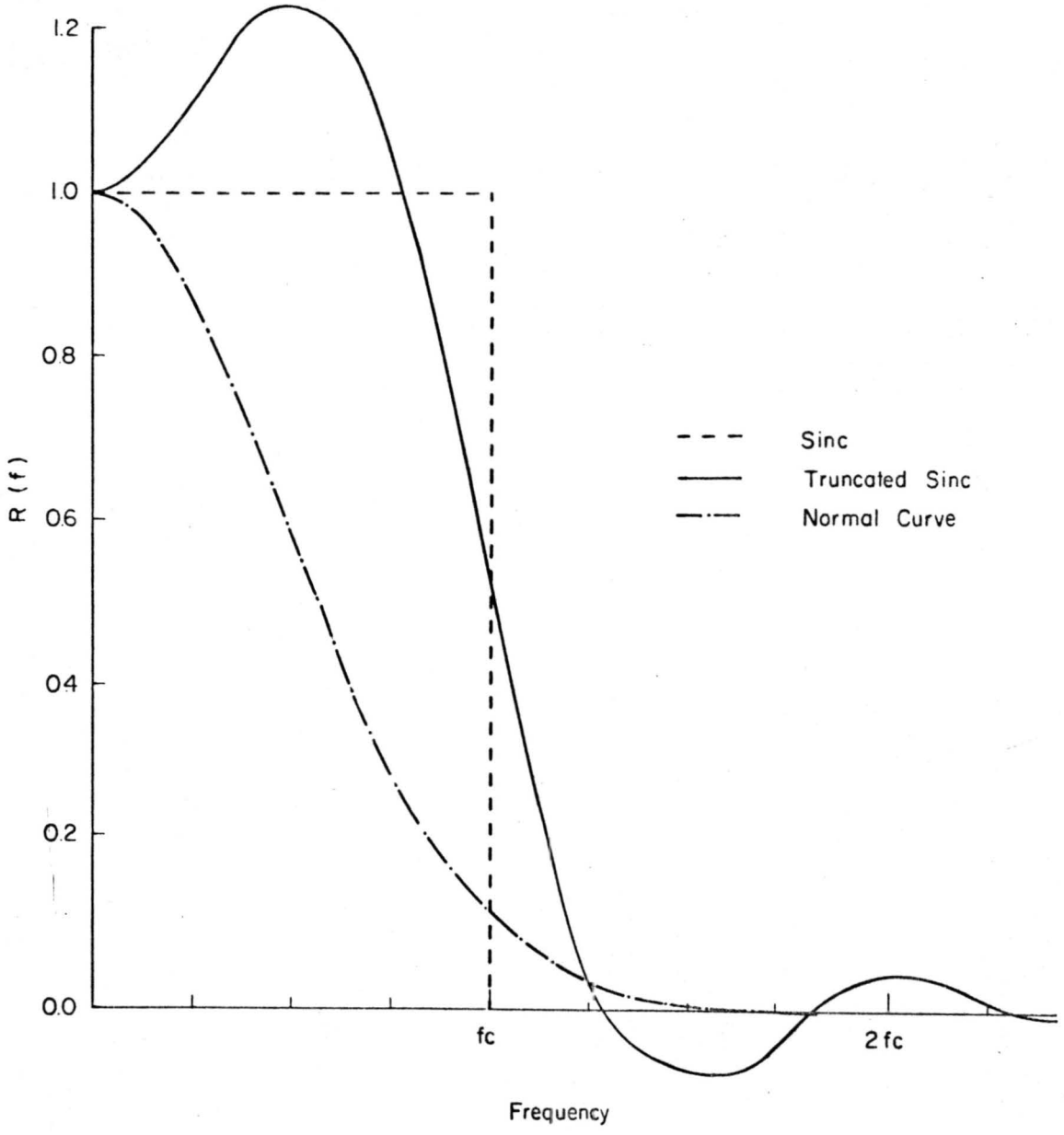

Fig. 2 Frequency response of Sinc, truncated Sinc and normal probability curves

For application to weather records, which are influenced by a solar cycle of about 11 years, Brier (1961) designed an empirical band pass filter function, which has a unit frequency response at a period of 11 years, decreasing to zero at 22 years and 5.5 years. By this particular weight function, he obtained a satisfactory analysis of weather records.

Besides Holloway and Brier, Wiener (1949), Blackman-Tukey (1958), Jenkins (1961), Parzen (1961), Goodman (1962) made important contributions to the development of optimum filter shapes.

None of these authors gave a further detailed discussion of the truncated Sinc function. Although this function oscillates about the zero axis and converges only slowly, a fairly good frequency response function can be obtained from it if it is truncated at a suitable distance from both sides of the origin. The limitation of the truncation distance is imposed by the number of data points discarded because of the filtering process, and by the computing time of the digital computer. For example, if the digitized time spacing of a time series is 0.025 seconds and the time series to be filtered out has a central frequency f Hz, then the number of points to be discarded is:

$$\frac{1}{0.025} \propto \left(\frac{\beta}{2} + 1\right) \frac{1}{f} \qquad (1\text{-}7)$$

where α is the ratio of the length of Sinc function to the length of the

main lobe of that function (cf. Sec. 2.1, Fig. 3), β is the band width in terms of the filtered central frequency f. Equation 1-3 shows that the smaller values of α, β and larger frequencies will give a smaller number of discarded points. Practically, if $f = 2$, $\beta = 1/4$, and $\alpha = 8$, the total number of discarded data points (corresponding to the length of the Sinc function) will be about 200. For a long piece of record, say 2000 points, the discarded points (100 points on both ends of the record) is a small portion, which is inversely proportional to the filtered central frequency.

Detailed calculation of the filter shape of the truncated Sinc function and its application will be discussed in later chapters.

Chapter II

THEORETICAL BACKGROUND

2.1 Filter Characteristics

2.1.1 Moving Average with Filter

Theoretically, the Fourier transform of Sinc function is a rectangular window. Based on this, the Sinc function is chosen to be the ideal low pass filter. If the length T_s of the main lobe of the Sinc function is suitably set, then by the definition of the running mean, the time series $\hat{x}_1(\omega_1, t)$, which consists of all different frequency components from zero up to ω_1, would be:

$$\hat{X}_1(\omega_1, t_j) = \lim_{T_o \to \infty} \frac{1}{T_o} \int_{T_j - \frac{T_o}{2}}^{T_j + \frac{T_o}{2}} y_1(t)\, \mathrm{Sinc}\left(\frac{t_j - t}{T_s}\right) dt$$

$$= \overline{y_1(t)\, \mathrm{Sinc}\left(\frac{t_j - t}{T_s}\right)} \quad , \tag{2-1}$$

where $\omega_1 = 2\pi/T_s$, and T_o is the length of the rectangular window (see Fig. 3). Furthermore, if the length of the main lobe of the Sinc function is changed to $(T_s + 2\Delta t)$, then

$$\hat{X}_2(\omega_2, t_j) = \overline{y_1(t)\, \mathrm{Sinc}\left(\frac{t_j - t}{T_s + 2\Delta t}\right)} \quad , \tag{2-2}$$

where $\omega_2 = \omega_1 - \Delta\omega = 2\pi/(T_s + 2\Delta t)$, and $\Delta\omega$ is the bandwidth.

The time series $\hat{x}_2(\omega_2, t)$ contains all frequencies from zero to ω_2, the rest are filtered out by the filter function. If we subtract

$\hat{x}_2$ from $\hat{x}_1$, the desired, filtered time function $x(\omega, t)$, which contains frequency components from ω_2 to ω_1 is then obtained:

$$x(\omega,t) = \hat{x}_1(\omega_1,t) - \hat{x}_2(\omega_2,t) \qquad (2\text{-}3)$$

If the bandwidth of the filter $\Delta\omega$, is small enough, then $x(\omega, t)$ could be considered to be a time series solely at a central frequency ω, $\omega = (\omega_1 + \omega_2)/2$.

2.1.2 Truncated Sinc Function

By introducing an ideal low pass filter (Sinc function) in the time domain, a spectrum in the frequency domain will be found which is flat from the very high frequency component down to the cutoff frequency. Practically, to obtain a true rectangular filter, the Sinc-function must be extended over a very long record, requiring practically an infinite length of a record of time series for the application of Sinc function. This is clearly impossible. Also, from an economic point of view, a short length of record is desired. For these two reasons, a moderate length of Sinc function is chosen, which is sufficiently long so as not to materially affect the accuracy.

In order to have a limited length of Sinc function, we are forced to introduce a rectangle function in Eq. (2-1) (see Fig. 3):

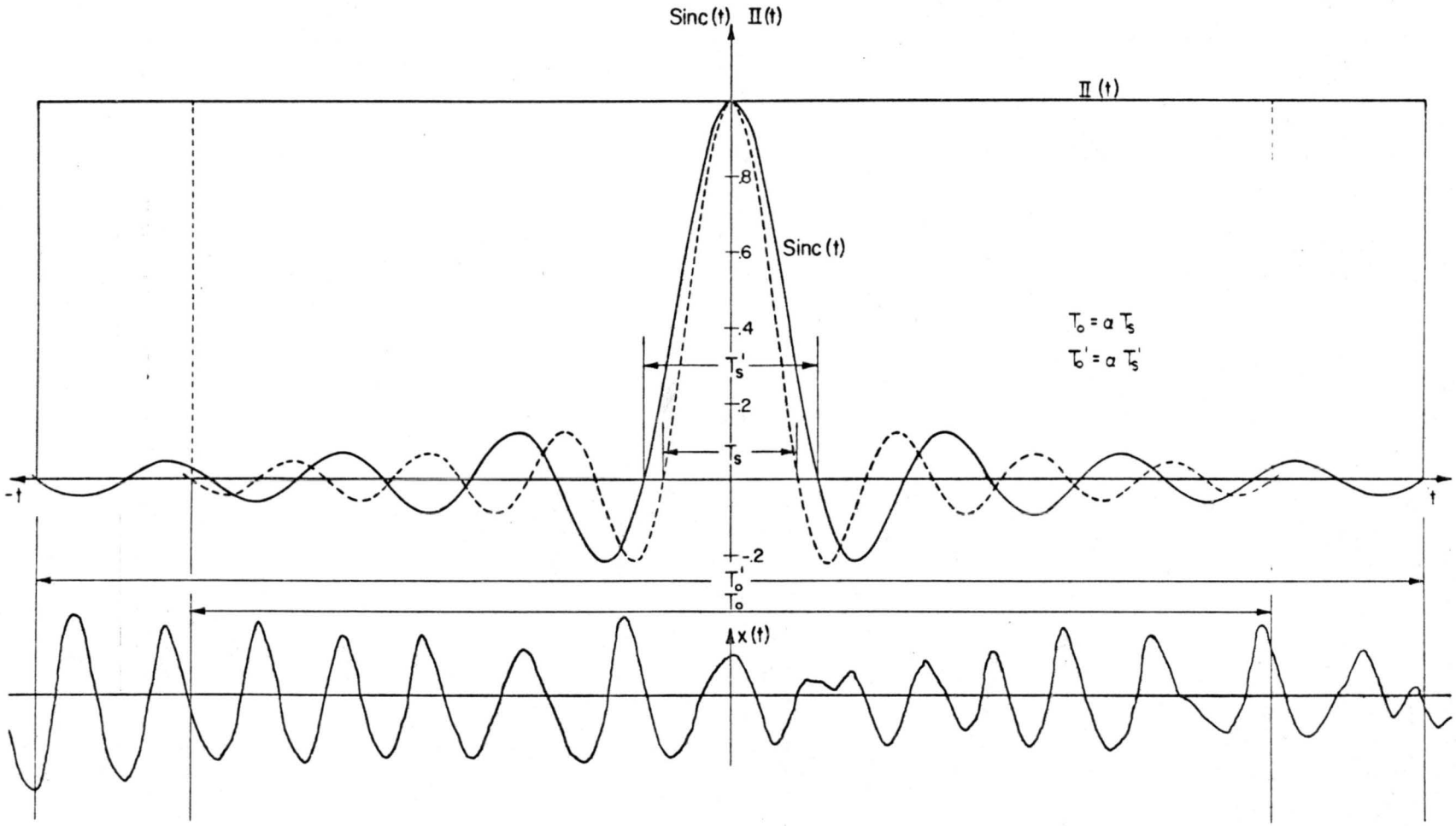

Fig. 3. Construction of band pass filter by truncated Sinc function.

$$\hat{X}_i(\omega_i, t_j) \approx \frac{1}{T_o} \int_{-\infty}^{\infty} y_i(x,t)\, \mathrm{Sinc}\left(\frac{t_j - t}{T_s}\right) \amalg \left(\frac{t_j - t}{T_o}\right) dt$$

$$\approx \frac{1}{T_o} \int_{t_j - \frac{T_o}{2}}^{t_j + \frac{T_o}{2}} y_i(x,t)\, \mathrm{Sinc}\left(\frac{t_j - t}{T_s}\right) dt \quad , \qquad (2\text{-}4)$$

Equation (2-4) is a convolution integral. Since the Fourier transform of the convolution of the two functions X and Y is equal to the product of the Fourier transforms of X and Y (see Ron Bracewell, "The Fourier Transform and Its Application", p. 111). The Fourier transform of Eq. (2-4) becomes:

$$A_x(\omega_i) = \left[A_x(\omega) \right] \mathrm{F.T.} \left(\mathrm{Sinc}\left(\frac{t_j - t}{T_s}\right) \amalg \left(\frac{t_j - t}{T_o}\right) \right) \quad . \qquad (2\text{-}5)$$

The width of the main lobe of the Sinc function is $(T_o + 2\,\Delta t)$. Then the Fourier transform of Eq. (2-4) becomes:

$$A_x(\omega_2) = \left[A_x(\omega) \right] \mathrm{F.T.} \left(\mathrm{Sinc}\left(\frac{t_j - t}{T_s + 2\Delta t}\right) \amalg \left(\frac{t_j - t}{T_o}\right) \right) \quad . \qquad (2\text{-}6)$$

The spectrum at central frequency $\omega\,(\omega = (\omega_1 + \omega_2)/2)$ is given by:

$$A_x(\omega_2 \sim \omega_1)$$

$$= A_x(\omega) \left\{ \mathrm{F.T.}\left[\mathrm{Sinc}\left(\frac{t_j - t}{T_s}\right) \amalg \left(\frac{t_j - t}{T_o}\right) \right] - \mathrm{F.T.}\left[\mathrm{Sinc}\left(\frac{t_j - t}{T_s + 2\Delta t}\right) \amalg \left(\frac{t_j - t}{T_o}\right) \right] \right\} \qquad (2\text{-}7)$$

This result is applied in this thesis for filtering wave data. The details of Eq. (2-7) are discussed in the remainder of this chapter.

2.1.3 Frequency Response of Truncated Sinc Function

Consider the function:

$$F(t) = \text{Sinc}\left(\frac{2t}{T_s}\right) \amalg \left(\frac{t}{T_o}\right)$$

The Fourier transform of this function is given by:

$$A_{\text{Sinc}}(\omega_i) = \int_{-\infty}^{\infty} \text{Sinc}\left(\frac{2t}{T_s}\right) \amalg \left(\frac{t}{T_o}\right) \exp(-i\omega t)\, dt$$

$$= \int_{-\frac{T_o}{2}}^{\frac{T_o}{2}} F(t) \exp(-i\omega t)\, dt \qquad (2\text{-}8)$$

As T_o approaches infinity:

$$A_{\text{Sinc}}(\omega) = \frac{T_s}{2} \amalg \left(\frac{1}{2}\right) \qquad (2\text{-}9)$$

where II(1/2) is a rectangular window with unit height and base. Actually, T_o is finite, so that

$$A_{\text{Sinc}}(\omega_i) = \frac{T_s}{2\pi}\left[\text{Si}\,\pi\left(\frac{T_o}{T_s} + \frac{T_o\omega}{2\pi}\right) + \text{Si}\,\pi\left(\frac{T_o}{T_s} - \frac{T_o\omega}{2\pi}\right)\right] \qquad (2\text{-}10)$$

where Si is a function discussed during the detailed derivation of Eq. (2-10) in Appendix 1.

Let $\alpha = T_o/T_s$

= ratio of length of rectangular function to the length of main lobe of the Sinc function.

Rewriting Eq. (2-10) in terms of α, we get:

$$A_{T_s}(\omega_i) = \frac{T_s}{2\pi}\left[\text{Si}\left(\pi\alpha + \frac{\alpha T_s\omega}{2}\right) + \text{Si}\left(\pi\alpha - \frac{\alpha T_s\omega}{2}\right)\right] \qquad (2\text{-}11)$$

Since $\omega T_s = 2\pi = \text{Const}$, then $\omega = 2\pi f = 2\pi/T_s$. For any value of T_s, the cutoff frequency ω is obtained.

2.1.4 Filter Shape and Error Estimation

If the length of the main lobe of the Sinc function T_s in Eq. (2-8) is changed to $T_s + 2\Delta T$, then Eq. (2-11) becomes:

$$A_{T_s}(\omega_2) = \frac{T_s+2\Delta t}{2\pi}\left[Si\left(\pi\alpha + \frac{\alpha(T_s+2\Delta t)\omega}{2}\right) + Si\left(\pi\alpha - \frac{\alpha(T_s+2\Delta t)\omega}{2}\right)\right] \tag{2-12}$$

and the filter shape (FS) is:

$$FS(\omega_2 \sim \omega_1) = A_{T_s}(\omega_1) - A_{T_s}(\omega_2) \tag{2-13}$$

To solve (2-13) numerically, we can rewrite (2-8) as:

$$A_{T_s}(\omega_1) = \frac{T_s}{2\pi}\left\{\left(\pi\alpha + \frac{\omega\alpha T_s}{2}\right)\left[1 - \frac{\left(\pi\alpha + \frac{\omega\alpha T_s}{2}\right)^2}{3\cdot 3!} + \frac{\left(\pi\alpha + \frac{\omega\alpha T_s}{2}\right)^4}{5\cdot 5!} - \cdots\right] + \left(\pi\alpha - \frac{\omega\alpha T_s}{2}\right)\left[1 - \frac{\left(\pi\alpha - \frac{\omega\alpha T_s}{2}\right)^2}{3\cdot 3!} + \frac{\left(\pi\alpha - \frac{\omega\alpha T_s}{2}\right)^4}{5\cdot 5!} - \cdots\right]\right\} \tag{2-14}$$

$$A_{T_s'}(\omega_2) = \frac{T_s'}{2\pi}\left\{\left(\pi\alpha + \frac{\omega\alpha T_s'}{2}\right)\left[1 - \frac{\left(\pi\alpha - \frac{\omega\alpha T_s'}{2}\right)^2}{3\cdot 3!} + \frac{\left(\pi\alpha - \frac{\omega\alpha T_s'}{2}\right)^4}{5\cdot 5!} - \cdots\right] + \left(\pi\alpha - \frac{\omega\alpha T_s'}{2}\right)\left[1 - \frac{\left(\pi\alpha - \frac{\omega\alpha T_s'}{2}\right)^2}{3\cdot 3!} + \frac{\left(\pi\alpha - \frac{\omega\alpha T_s'}{2}\right)^4}{5\cdot 5!} - \cdots\right]\right\} \tag{2-15}$$

where $T_s = T_s + 2\Delta t$, and the filter shape will become:

$$FS(\omega_2 \sim \omega_1) = A_{T_s}(\omega_1) - A_{T_s'}(\omega_2)$$

$$= \frac{T_s}{2\pi}\left\{(\pi\alpha + \frac{\omega\alpha T_s}{2})\left[1 - \frac{(\pi\alpha + \frac{\omega\alpha T_s}{2})^2}{3\cdot 3!} + \frac{(\pi\alpha + \frac{\omega\alpha T_s}{2})^4}{5\cdot 5!} - \cdots\right]\right.$$

$$\left. + (\pi\alpha - \frac{\omega\alpha T_s}{2})\left[1 - \frac{(\pi\alpha - \frac{\omega\alpha T_s}{2})^2}{3\cdot 3!} + \frac{(\pi\alpha - \frac{\omega\alpha T_s}{2})^4}{5\cdot 5!} - \cdots\right]\right\}$$

$$- \frac{T_s'}{2\pi}\left\{(\pi\alpha + \frac{\omega\alpha T_s'}{2})\left[1 - \frac{(\pi\alpha + \frac{\omega\alpha T_s'}{2})^2}{3\cdot 3!} + \frac{(\pi\alpha + \frac{\omega\alpha T_s'}{2})^4}{5\cdot 5!} - \cdots\right]\right.$$

$$\left. + (\pi\alpha - \frac{\omega\alpha T_s'}{2})\left[1 - \frac{(\pi\alpha - \frac{\omega\alpha T_s'}{2})^2}{3\cdot 3!} + \frac{(\pi\alpha - \frac{\omega\alpha T_s'}{2})^4}{5\cdot 5!} - \cdots\right]\right\} \qquad (2\text{-}16)$$

For a detailed derivation of Eq. 2-16 see Appendix 2.

2.2 Practical Consideration During Filter Application

2.2.1 Filter Function (Sinc Function)

The Sinc function curve is computed from its definition:

$$\text{Sinc}(x) = \frac{\text{Sin}(\pi x)}{\pi x}$$

where $\pi = 3.141592654$. The computer program for Eq. (4.2) is shown in Appendix 3 and its results are shcwn in Table 1. Comparison of these computed results and those given in mathematical tables shows that the errors are less than 0.1%. The computed Sinc function curves for central frequency equals 1 Hz are shown in Fig. 3.

Table 1. Computer results of Sinc function

SINC(M)=				
6.1856693E-03	-4.6986894E-03	-1.5468180E-02	-2.5305133E-02	-3.3443910E-02
-3.9229632E-02	-4.2169919E-02	-4.1975617E-02	-3.8587236E-02	-3.2184801E-02
-2.3179994E-02	-1.2190784E-02	-1.3051506E-10	1.2499411E-02	2.4368712E-02
3.4692707E-02	4.2649050E-02	4.7572366E-02	4.9008285E-02	4.6753124E-02
4.0875890E-02	3.1720513E-02	1.9887660E-02	6.1958226E-03	-8.3688464E-03
-2.2731519E-02	-3.5796664E-02	-4.6534505E-02	-5.4059052E-02	-5.7698772E-02
-5.7053449E-02	-5.2032619E-02	-4.2872206E-02	-3.0127452E-02	-1.4641964E-02
2.5056214E-03	2.0074115E-02	3.6746701E-02	5.1226399E-02	6.2333358E-02
6.9096915E-02	7.0835520E-02	6.7218283E-02	5.8303007E-02	4.4547109E-02
2.6789661E-02	6.2047966E-03	-1.5771220E-02	-3.7534978E-02	-5.7426973E-02
-7.3851372E-02	-8.5396242E-02	-9.0945642E-02	-8.9775536E-02	-8.1625201E-02
-6.6739456E-02	-4.5876084E-02	-2.0277243E-02	8.3947245E-03	3.8154972E-02
6.8820663E-02	9.2156366E-02	1.1203047E-01	1.2457281E-01	1.2832284E-01
1.2235807E-01	1.0639329E-01	8.0842742E-02	4.8839602E-02	6.2095840E-03
-3.8601541E-02	-8.4643794E-02	-1.2861662E-01	-1.6705209E-01	-1.9651743E-01
-2.1382486E-01	-2.1623621E-01	-2.0164952E-01	-1.6875570E-01	-1.1715475E-01
-4.7423464E-02	3.8870977E-02	1.3921362E-01	2.5023965E-01	3.4789301E-01
4.8756829E-01	6.0443551E-01	7.1358549E-01	8.1033196E-01	8.9044615E-01
9.5037976E-01	9.8745347E-01	1.0000000E+00	9.8745347E-01	9.5037976E-01
8.9044615E-01	8.1033196E-01	7.1358549E-01	6.0443551E-01	4.8756829E-01
3.4788301E-01	2.5023965E-01	1.3921362E-01	3.8870977E-02	-4.7423464E-02
-1.1715475E-01	-1.6875570E-01	-2.0164952E-01	-2.1623621E-01	-2.1382486E-01
-1.9651743E-01	-1.6705209E-01	-1.2861662E-01	-8.4643794E-02	-3.8601541E-02
6.2095840E-03	4.8839602E-02	8.0842742E-02	1.0639329E-01	1.2235807E-01
1.2832284E-01	1.2457281E-01	1.1203047E-01	9.2156366E-02	6.8820663E-02
3.8154972E-02	8.3947245E-03	-2.0277243E-02	-4.5876084E-02	-6.6739456E-02
-8.1625201E-02	-8.9775536E-02	-9.0945642E-02	-8.5396242E-02	-7.3851372E-02
-5.7426973E-02	-3.7534978E-02	-1.5771220E-02	6.2047966E-03	2.6789661E-02
4.4547109E-02	5.8303007E-02	6.7218283E-02	7.0835520E-02	6.9096915E-02
6.2333358E-02	5.1226399E-02	3.6746701E-02	2.0074115E-02	2.5056214E-03
-1.4641964E-02	-3.0127452E-02	-4.2872206E-02	-5.2032619E-02	-5.7053449E-02
-5.7698772E-02	-5.4059052E-02	-4.6534505E-02	-3.5796664E-02	-2.2731519E-02
-8.3688464E-03	6.1958226E-03	1.9887660E-02	3.1720513E-02	4.0875890E-02
4.6753124E-02	4.9008285E-02	4.7572366E-02	4.2649050E-02	3.4692707E-02
2.4368712E-02	1.2499411E-02	-1.3051506E-10	-1.2190784E-02	-2.3179994E-02
-3.2184801E-02	-3.8587236E-02	-4.1975617E-02	-4.2169919E-02	-3.9229632E-02
-3.3443910E-02	-2.5305133E-02	-1.5468180E-02	-4.6986894E-03	6.1856693E-03

SINC(M)=				
1.2143601E-02	-1.5645429E-03	-1.5468180E-02	-2.7834974E-02	-3.7074011E-02
-4.1937447E-02	-4.1685516E-02	-3.6193504E-02	-2.5985814E-02	-1.2190784E-02
3.3805455E-03	1.9419094E-02	3.3345049E-02	4.3551179E-02	4.8632742E-02
4.7752885E-02	4.0875890E-02	2.8580767E-02	1.2231764E-02	-6.2747698E-03
-2.4702507E-02	-4.0733866E-02	-5.2280887E-02	-5.7698772E-02	-5.6061239E-02
-4.7276434E-02	-3.2138445E-02	-1.2266504E-02	1.0059522E-02	3.2151519E-02
5.1226399E-02	6.4744841E-02	7.0735530E-02	6.8065089E-02	5.6618652E-02
3.7365279E-02	1.2294972E-02	-1.5771220E-02	-4.3481427E-02	-6.7333102E-02
-8.4091859E-02	-9.1201285E-02	-8.7134812E-02	-7.1645093E-02	-4.5876084E-02
-1.2317141E-02	2.5404433E-02	6.2877688E-02	9.5377077E-02	1.1839962E-01
1.2821359E-01	1.2235807E-01	1.0003515E-01	6.2345513E-02	1.2332991E-02
-4.5177610E-02	-1.0394325E-01	-1.5583852E-01	-1.9651743E-01	-2.1613915E-01
-2.1008606E-01	-1.7460120E-01	-1.0827726E-01	-1.2342506E-02	1.0929240E-01
2.5023965E-01	4.0207969E-01	5.5501093E-01	6.9864658E-01	8.2288624E-01
9.1878104E-01	9.7931094E-01	1.0000000E+00	9.7931094E-01	9.1878104E-01
8.2288624E-01	6.9864658E-01	5.5501093E-01	4.0207969E-01	2.5023965E-01
1.0929240E-01	-1.2342506E-02	-1.0827726E-01	-1.7460120E-01	-2.1008606E-01
-2.1613915E-01	-1.9651743E-01	-1.5583852E-01	-1.0394325E-01	-4.5177610E-02
1.2332991E-02	6.2345513E-02	1.0003515E-01	1.2235807E-01	1.2821359E-01
1.1839962E-01	9.5377077E-02	6.2877688E-02	2.5404433E-02	-1.2317141E-02
-4.5876084E-02	-7.1645093E-02	-8.7134812E-02	-9.1201285E-02	-8.4091859E-02
-6.7333102E-02	-4.3481427E-02	-1.5771220E-02	1.2294972E-02	3.7365279E-02
5.6618652E-02	6.8065089E-02	7.0735530E-02	6.4744841E-02	5.1226399E-02
3.2151519E-02	1.0059522E-02	-1.2266504E-02	-3.2138445E-02	-4.7276434E-02
-5.6061239E-02	-5.7698772E-02	-5.2280887E-02	-4.0733866E-02	-2.4702507E-02
-6.2747698E-03	1.2231764E-02	2.8580767E-02	4.0875890E-02	4.7752885E-02
4.8632742E-02	4.3551179E-02	3.3345049E-02	1.9419094E-02	3.3805455E-03
-1.2190784E-02	-2.5985814E-02	-3.6193504E-02	-4.1685516E-02	-4.1937447E-02
-3.7074011E-02	-2.7834974E-02	-1.5468180E-02	-1.5645429E-03	1.2143601E-02

2.2.2 Filter Shape

One of the main objectives of this study was to calculate the frequency response of the truncated Sinc function. This was attempted by two different methods. First, a combination of Si function can be obtained in current mathematical tables for only a short range of frequencies (See Standard Mathematical Tables, p. 356). The author was, therefore, forced to adopt a numerical method. As detailed in Appendix 2, the Fourier transform of the truncated Sinc function was first expanded about the origin and then integrated. The computer program for the solutions of Eq. (2-14) and Eq. (2-15) is shown in Appendix 4. Because of the limited capacity of the CDC 6400 digital computer of Colorado State University, the frequency responses of the truncated Sinc functions could be calculated only up to the cutoff frequencies with the results shown by the solid curves in Fig. 4. The computed results of each term of the power series of Eq. (2-14) and (2-15) showed that this infinite series diverged roughly for the first 50 terms and then converged. For calculated frequencies greater than the cutoff frequency, the maximum value of the first terms of the series before convergence is always greater than 10^{30}, while the number of significant digits of the computer is only 28 (at double precision). Thus, during the calculations, if the value of any term is greater than 10^{24}, part of the value will be neglected by the computer because it calculates by mantissa. This caused the results to be inaccurate beyond the cutoff frequency.

As a second approach, the author tried to expand the power series of Eq. (2-14) around the cutoff frequency in order to obtain a better estimation of the frequency response beyond cutoff. However, this proved fruitless because the expansion was found to be most complicated and was finally abandoned.

Theoretically, the Fourier transform of the truncated Sinc function beyond the cutoff of frequency should oscillate about the zero axis and die out at larger frequencies as shown by the dashed curves in Fig. 4. Hence, no error estimation of the filter shape can be given. The solid curve in Fig. 5 is the calculated band pass filter shape obtained with the present limited computer capacity, while the dashed curve in that figure is the estimated theoretical filter shape. Some day, when a computer with a greater number of significant digits is available, the shape of the band pass filter can be obtained, and thus a precise error estimation can be given.

The Fourier transform of the Sinc function is a rectangular window. Intuitively, the longer the truncated Sinc function is, the less the error will be, as shown in Fig. 6 (for $\alpha = 4$, and $\alpha = 6$). The computed results for several cases indicated the above hypothesis. The number of oscillations in the frequency response curves were found to be always $\alpha/2$. They largely affect the errors of the filter. A larger α has larger number of oscillations and smaller errors.

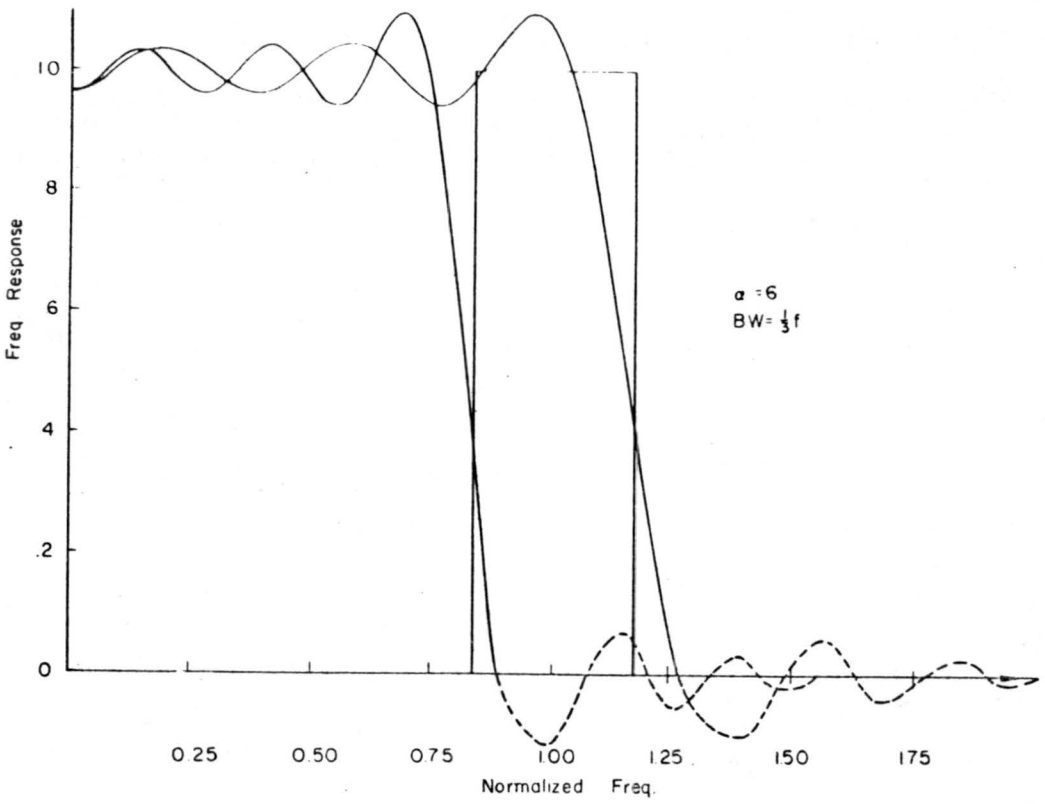

Fig. 4 Fourier transform of truncated Sinc function

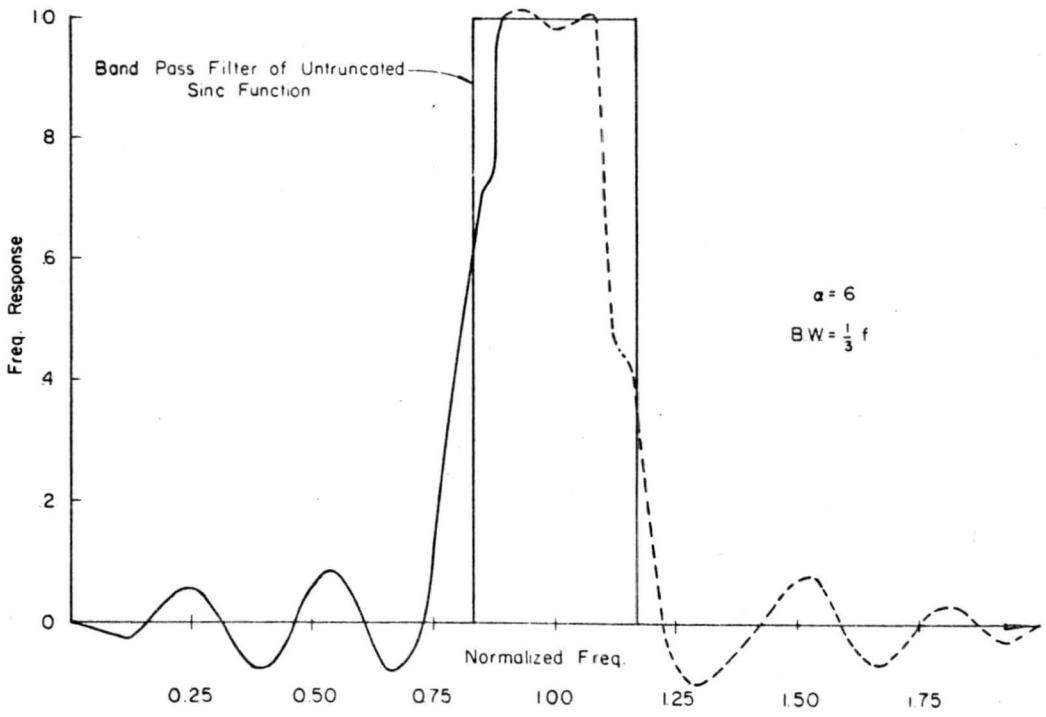

Fig. 5 Calculated and estimated band pass filter shape

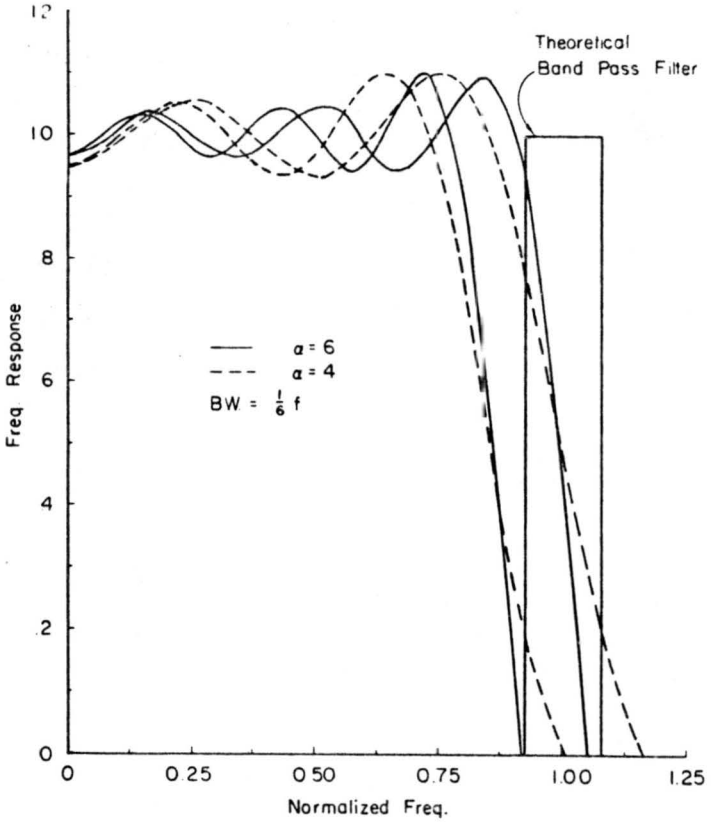

Fig. 6 Comparison of frequency response of various length of truncated Sinc functions

The band width of the filter also affects the precision of the filter. Theoretically, the best band pass filter is one with a minimum band width. The computer results indicated that the normalized filter shape is independent of frequency. Furthermore, if $2/\alpha$ is employed for the constant ratio band width of the frequency, the best filter shape was obtained (Figs. 4, 5, 6). If the band width is much greater than $(2/\alpha)f$, the filtered time series will be interfered with by other frequency components. If it is too small, large errors will be introduced because of the large side lobes of the low pass filter shape (Fig. 6). Experimentally, $2/\alpha$ is chosen for the constant ratio band width.

For the spectrum and correlation calculations, $\alpha = 8$ and a band width of $(1/4)f$ were used. Undoubtedly, the band pass filter shape is much better than that shown in Fig. 5 ($\alpha = 6$, B.W. = 1/3f), but the limitations mentioned above of the computer do not permit a comparison.

2.2.3 Choice of Time Steps

The time spacing between adjacent points is 0.025 seconds for the manually digitized data. This time spacing is small enough for low frequency waves, but for high frequency components, such a large time spacing might lose some information of wave energy. This phenomenon can be seen in Fig. 10: there are some phase shifts in the filtered data at large t. Theoretically, the period of

a certain particular frequency component must be constant. The phase shift might be caused by the interference of higher or lower frequency components around the filtered central frequency, because a certain band width is used. If the data is digitized by ADDCS (Chapter 3.3), the time spacing can be chosen as small as 0.000015 seconds. With such small time spacings, the present technique can also be applied to high frequency air turbulence studies.

2.3 Applications

2.3.1 Space-Time Correlation

For progressive waves, the irrotational propagation speed of infinitesimal gravity, deep water waves of frequency f is given as:

$$c \approx \sqrt{\frac{g}{K}} = \frac{g}{2\pi f} \quad , \tag{2-17}$$

where c is wave speed, K is wave number and f is frequency. Theoretically, according to equation (2-17), the wave speed is inversely proportional to the frequency. The wave speed was actually measured by the following technique involving space-time correlations.

As shown in Fig. 7, wave data are taken simultaneously with two probes a distance δ apart along the direction of wave motion, then the cross-correlation function, or the space-time correlation, of these time series is given as:

$$\psi(\delta,\tau) = \lim_{T\to\infty} \frac{1}{2T} \int_{-T}^{T} y_1(x,t)\, y_2(x+\delta, t+\tau)\, dt$$

$$\doteq \overline{y_1(x,t)\, y_2(x+\delta, t+\tau)} \,, \qquad (2\text{-}18)$$

where $y_1(x, t)$ and $y_2(x + \delta, t)$ are time series measured with the upstream and downstream probes respectively.

The correlation coefficient is given as:

$$R_{y_1 y_2}(\delta,\tau) = \frac{\psi(\delta,\tau)}{\sigma_1(x,t)\, \sigma_2(x+\delta, t+\tau)} \,, \qquad (2\text{-}19)$$

where σ_1 and σ_2 are the standard deviations of y_1 and y_2 respectively.

Although the shapes of water waves vary not only in time but also in space, their propagation speed can be obtained from the space-time correlation curves, if the distance δ, between the two probes is not too large:

$$C = \frac{\delta}{\tau} \qquad (2\text{-}20)$$

where τ is the time delay of the maximum cross correlation coefficient. If a particular frequency component of time series y_{1_f} and y_{2_f} can be identified (filtered out) from the original time series y_1 and y_2 respectively, then the propagation speed of that particular frequency component can be obtained in the same way.

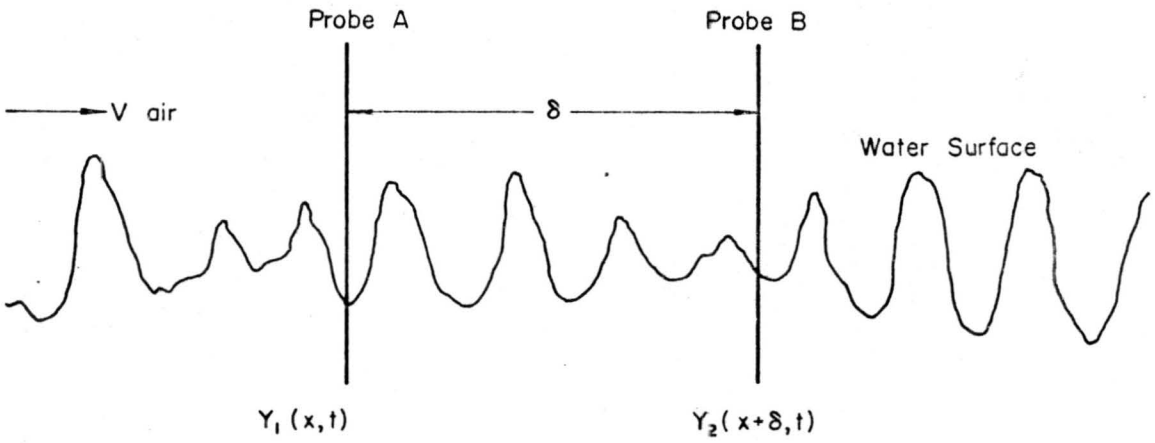

Fig. 7 Experimental set-up of space-time correlation

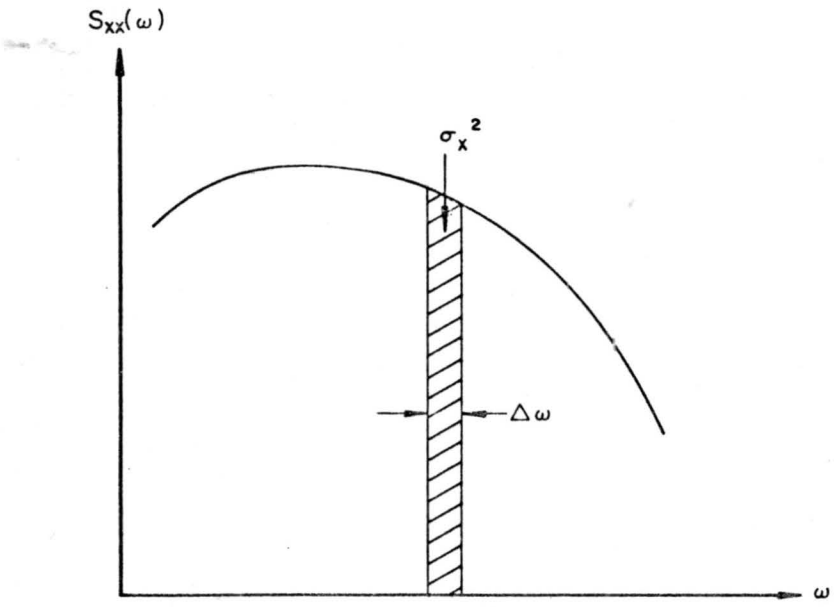

Fig. 8 Spectrum density of random time function

2.3.2 Spectrum Analysis

By taking the Fourier transform of the auto-correlation function, the frequency spectrum of water waves is obtained.

$$S_{xx}(\omega) = \frac{1}{2\pi}\int_{-\infty}^{\infty} R_{xx}(\tau)\exp(-i\omega\tau)\,d\tau$$

Since $S_{xx}(\omega)$ is real and $R_{xx}(\tau)$ is even, the Wiener-Khintchine relations yield: (see Y. W. Lee, "Statistical Theory of Communication," pp. 56-58)

$$S_{xx}(\omega) = \frac{1}{\pi}\int_{0}^{\infty} R_{xx}(\tau)\cos(\omega\tau)\,d\tau \quad , \tag{2-21}$$

where $S_{xx}(\omega)$ is the frequency spectrum, and $R_{xx}(\tau)$ the auto-correlation of y_1 or y_2.

The band pass filter of this study gives a means of reducing the side lobe leakages of a low pass filter and to make a more accurate spectrum estimation than, say, the Blackman-Tukey method. This follows from the definition of the spectrum, according to which the variances associated with the frequencies lying in the spectral band $d\omega$ with center frequency ω are given as

$$\sigma_{\omega}^2 = S_{xx}(\omega)\,d\omega \tag{2-22}$$

Consequently, the total variance is

$$\sigma_x^2 = \int_{-\infty}^{\infty} S_{xx}(\omega)\, d\omega = \int_{-\infty}^{\infty} d(\sigma_\omega^2) \qquad (2\text{-}23)$$

Thus, the power spectrum can be interpreted in terms of variances of uncorrelated data. If the uncorrelated data is a filtered stationary random time function at a particular frequency, then the variance would be the spectrum associated with the frequency lying in that spectral band (see Fig. 8).

For both filtered space-time correlations and spectrum analysis, one faces the same problem, namely, how to filter a particular frequency component ω out of a stationary time function.

So, the spectral density associated with a central frequency ω and a band width $\Delta\omega$ is obtained by:

$$S_{xx}(\omega) = n \frac{\sigma_\omega^2}{\Delta\omega} = \frac{n}{\Delta\omega} \left(\overline{x^2(\omega, t)} - m^2 \right) , \qquad (2\text{-}24)$$

where $m = \overline{x(t)}$, and n is the scale factor, obtained by dividing the total spectrum and the accumulated spectrum density.

Chapter III

3.1 Wind-water Tunnel

The experiments were performed in the wind tunnel flume combination located in the Fluid Dynamics and Diffusion Laboratory of Colorado State University. The wind water tunnel, shown in Fig. (9), has been described in detail by Plate (1965). It contains a truss-supported plexiglas channel of the test section about 12 meters long, and 0.61 meters wide by 0.76 meters high. The inlet section, where the water enters the facility, consists of honeycomb screens, which serve as diffusers for the incoming water. The sloping aluminum honeycomb beach at the outlet acts as a wave dissipating beach. A smoothly sanded aluminum flat plate, standing 10.6 cm above the floor of the tunnel is extended from the inlet of the tunnel to 5.0 m of the test section. The plate is introduced so that the air flow can develop to an equilibrium condition while approaching the water surface. The water is blocked by a vertical aluminum wall at the junction point for obtaining standing water. When the air blows, the water depth is adjusted so that a smooth and continuous transition from the plate to the water surface is provided. An axial fan draws the air through a fiberglas inlet bell and a set of screens, into a contraction section and the air smoothly enters the test section through a honeycomb screen. The outlet is a fan section, which is

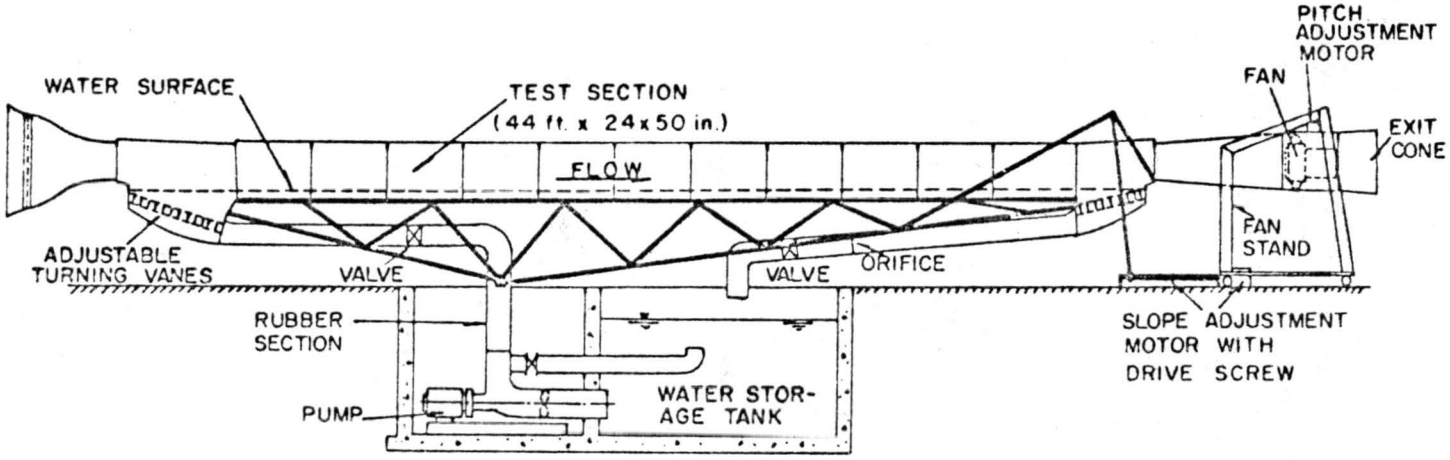

Fig. 9 Schematic diagram of CSU wind-water tunnel

supported independently of the test section. If it is desirable, the inlet bell and fan section can be exchanged to reverse the air flow direction.

3.2 Measurement of Water Surface Displacement

The water surface displacement was measured with a capacitance gauge, which consisted of a 32-gauge, nyclad insulated magnet wire, stretched vertically across the tunnel in the center of the cross section, and a bridge circuit developed in the Engineering Research Laboratories, at Colorado State University. The wire is not free of capillary adhesion effects. To eliminate this effect, the wire was submerged in water for more than one day and it was calibrated before and after each series of experiments. The water and the magnet wire were connected to the bridge circuit. Together they acted as a condensor whose capacitance varied proportionally to the water elevation. The bridge circuit gives a voltage output, which is fed to a brush recorder or an Ampex F. M. tape recorder.

3.3 Digitization of Data

Two sets of data were used in this work. Set I was taken by Chang and the author for spectrum estimation only. It contains the two cases listed in Table (3.3.1).

Table 3.3.1

Case	Fetch (m)	Reference Air Velocity (mps)
1	8.5	7.7
2	8.5	9.8

These data were recorded on magnetic tape, and were digitized by the Analog to Digital Data Conversion System (ADDCS), Model 751, produced by the Electronic Engineering Company of California at the National Bureau of Standards, Boulder, Colorado. The time spacing between succeeding points was chosen to be 0.0006 seconds. Details of this technique have been described by Chang (1968). The digitized data of the water waves were pre-smoothed before filtering by taking an equal weight running mean of every 25 data points first. This process removes most of the noise picked up by the signal during the measuring, recording and digitizing process, but retains the real energy produced by the water waves as stated by Chang (1968). After the smoothing procedure, the time spacing becomes 0.0006 x 25 = 0.015 seconds.

Data set II was taken for both spectrum and space-time correlation analysis. Four different cases of data were taken from simultaneous measurements with two probes, as tabulated in Table (3.3.2).

Table 3.3.2

Case	Fetch (m)	Reference Air Velocity (mps)	Distance Between Two Probes (cm)
1	3.5	10.67	6.35
2	9.0	10.67	13.21
3	9.0	10.67	31.5
4	9.0	10.67	59.37

These data were recorded on a Brush Mark III strip chart recorder and were digitized manually with 0.025 seconds time spacing in the Engineering Research Laboratories, Colorado State University. A filtered time series of a particular frequency component was then obtained by taking a running mean of the Sinc function from the original digitized data. Once the data was filtered it was ready for space-time correlation and spectrum estimation by calculating cross correlation coefficients and variance. All the statistical analyses were performed on the CDC 6400 digital computer of Colorado State University.

Chapter IV

EXPERIMENTAL RESULTS AND DATA ANALYSIS

4.1 Geometry of the Water Surface

Figure 10 is a typical record of unfiltered water surface displacement, which shows how the water waves vary continuously and irregularly with time. The waves appear in groups which usually contain about 6 to 10 waves of nearly constant frequency. The appearance of a modulation envelope means that the waves oscillate many times while their maximum amplitude slowly decreases and then increases as a consequence of the interference among several Fourier components.

Filtered water surface displacements of corresponding to particular frequency components of case 1, data II are shown in Fig. 10 and Fig. 11 for frequencies equal to 1, 4, 7, and 9, respectively. For a fixed particular frequency component, the period remains the same throughout the whole record, as demonstrated in the figures. Nearly regular modulated envelopes also appear in the filtered data.

The spectrum showed that the dominant frequency of this case lies at about 4 Hz. This property also can be easily seen from the comparison of the filtered time series. At the dominant frequency, the average wave amplitude occurs to be the maximum, while for either higher or lower frequencies than the dominant one, the

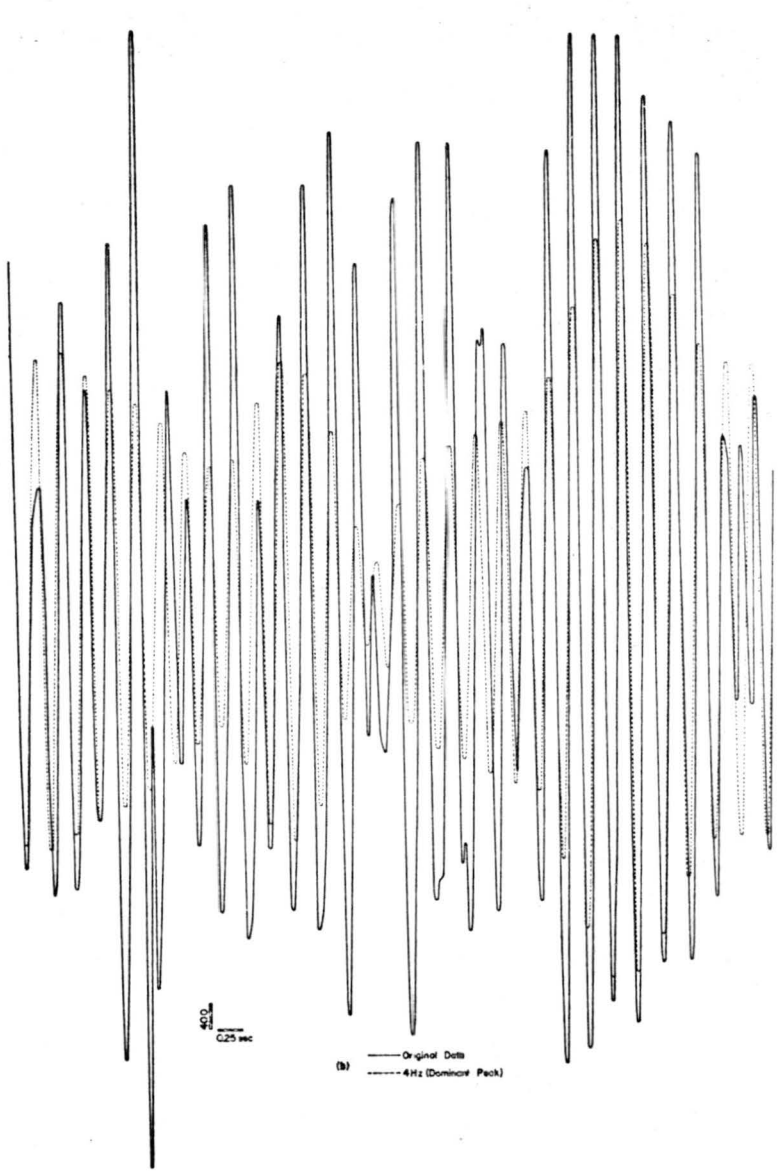

Fig. 10 Original and filtered water surface displacement

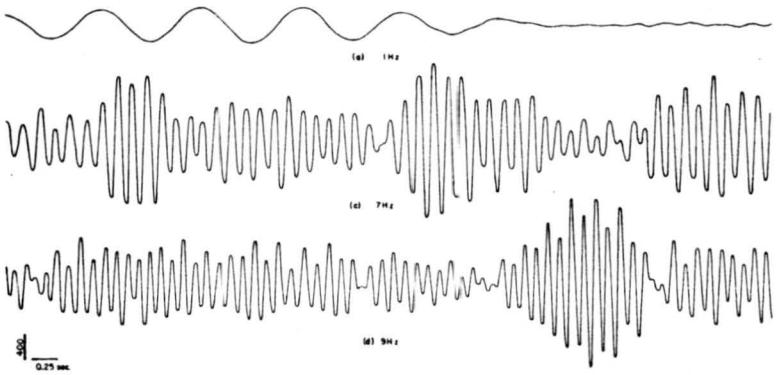

Fig. 11 Filtered water surface displacement

amplitudes are smaller than that of the dominant frequency. Furthermore, the larger the deviation from the dominant frequency, the smaller is the amplitude.

From the spectrum estimation (4.2), the scale factor n (Eq. 2-11) is found to be 155.7, thus the amplitude scale factor of filtered time series is $(155.7)^{1/2} = 12.48$. Comparison of the original data and the plotted, filtered time series at dominant frequency with the correction due to the scale factor included, showed that the average amplitude at the dominant frequency is about 0.85 of that of the original time series. The variance associated with spectrum at center frequency 4 Hz, and 4/3 Hz of band width is about 0.7 of the total variance. The square root of this value (0.7) is very close to the amplitude scale factor, as it should be. Calculation of the scale factor and the spectrum density curve in rectangular coordinate is shown in Fig. 12. The original and filtered time series at frequencies equal to 1, 4, 7, and 9 Hz are shown in Tables 2 through 6. The amplitudes of the filtered time series are equal to amplitudes of presented time series times 12.48.

Comparison of original time series with the filtered time series showed close correspondence at the frequency of the spectral peak. Records corresponding to other frequency components, showed quite different configuration than the original record.

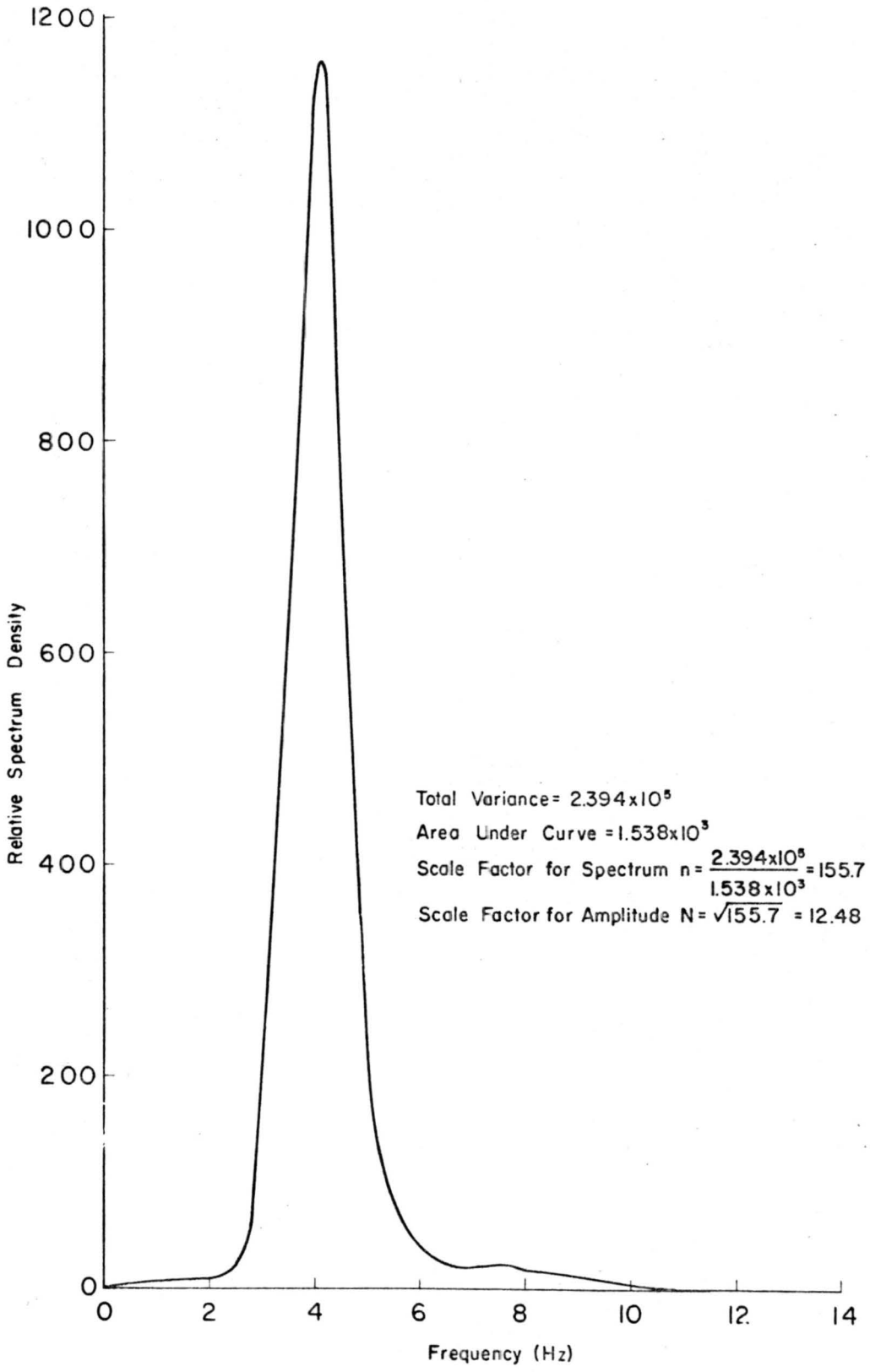

Fig. 12 Calculation of scale factor

Table 2. Unfiltered time series, Case 1 data II

X(M) =

6.659E+02	3.609E+02	2.393E+01	-2.971E+02	-4.581E+02	-5.141E+02	-4.251E+02	-9.107E+01	1.369E+02	1.809E+02
2.099E+02	2.199E+02	1.409E+02	-6.072E+00	-2.891E+02	-4.591E+02	-5.661E+02	-5.021E+02	-1.181E+02	4.659E+02
5.789E+02	3.899E+02	6.693E+01	-3.051E+02	-5.451E+02	-5.541E+02	-4.761E+02	-2.681E+02	2.679E+02	4.079E+02
3.149E+02	5.093E+01	-2.401E+02	-3.981E+02	-4.231E+02	-3.781E+02	-1.681E+02	1.859E+02	6.909E+02	5.769E+02
2.259E+02	-1.561E+02	-5.511E+02	-7.821E+02	-8.831E+02	-7.991E+02	-4.341E+02	2.369E+02	1.105E+03	1.054E+03
6.069E+02	7.993E+01	-4.691E+02	-8.931E+02	-1.092E+03	-2.411E+02	-5.741E+02	-7.471E+02	-6.501E+02	-4.391E+02
-5.907E+01	4.049E+02	3.329E+02	1.569E+02	7.928E+00	-1.641E+02	-3.111E+02	-2.851E+02	1.093E+01	1.969E+02
7.193E+01	-1.641E+02	-3.931E+02	-4.721E+02	-4.021E+02	-1.461E+02	2.729E+02	7.269E+02	5.409E+02	1.229E+02
-2.541E+02	-5.251E+02	-5.991E+02	-5.451E+02	-3.311E+02	-1.511E+02	2.349E+02	8.039E+02	7.799E+02	4.029E+02
-3.107E+01	-4.141E+02	-6.511E+02	-7.041E+02	-5.811E+02	-4.331E+02	-7.807E+01	1.939E+02	7.193E+01	-1.791E+02
-3.881E+02	-4.761E+02	-4.081E+02	-1.481E+02	2.479E+02	7.269E+02	5.479E+02	1.189E+02	-2.441E+02	-5.171E+02
-5.951E+02	-5.531E+02	-3.371E+02	-1.521E+02	2.279E+02	8.029E+02	7.719E+02	3.749E+02	-6.107E+01	-4.251E+02
-6.331E+02	-7.051E+02	-5.821E+02	-4.531E+02	-1.121E+02	6.479E+02	9.079E+02	6.729E+02	2.909E+02	-1.651E+02
-4.791E+02	-7.081E+02	-7.981E+02	-6.301E+02	-1.611E+02	4.949E+02	6.519E+02	4.279E+02	1.759E+02	-9.707E+01
-2.611E+02	-1.601E+02	4.993E+01	-5.007E+01	-1.991E+02	-2.611E+02	-2.841E+02	-2.931E+02	-1.931E+02	-6.107E+01
6.429E+02	7.769E+02	5.929E+02	2.629E+02	-2.171E+02	-5.651E+02	-8.051E+02	-8.621E+02	-7.381E+02	-3.951E+02
3.589E+02	8.849E+02	7.149E+02	3.579E+02	-5.407E+01	-3.991E+02	-5.691E+02	-5.761E+02	-5.371E+02	-5.331E+02
-3.491E+02	6.193E+01	6.309E+02	8.849E+02	5.589E+02	1.519E+02	-2.751E+02	-5.071E+02	-4.661E+02	-5.471E+02
-6.361E+02	-5.771E+02	-2.281E+02	2.569E+02	5.019E+02	4.869E+02	5.229E+02	3.199E+02	-3.807E+01	-2.661E+02
-5.091E+02	-5.971E+02	-5.621E+02	-6.007E+01	4.939E+02	4.429E+02	1.519E+02	-1.041E+02	-1.941E+02	-3.301E+02
-1.231E+02	6.193E+01	2.189E+02	2.539E+02	2.429E+02	9.928E+00	-2.771E+02	-4.931E+02	-5.781E+02	-5.281E+02
-5.107E+01	8.039E+02	8.699E+02	6.019E+02	2.029E+02	-2.661E+02	-6.541E+02	-8.691E+02	-8.941E+02	-6.061E+02
3.459E+02	1.090E+03	9.199E+02	4.679E+02	-4.307E+01	-4.661E+02	-7.391E+02	-8.621E+02	-7.791E+02	-2.811E+02
9.319E+02	1.093E+03	7.739E+02	2.609E+02	-2.441E+02	-6.131E+02	-7.711E+02	-6.951E+02	-4.381E+02	4.299E+02
1.092E+03	9.769E+02	5.049E+02	-5.807E+01	-4.551E+02	-7.151E+02	-8.141E+02	-6.531E+02	-2.191E+02	5.809E+02
9.719E+02	8.279E+02	5.079E+02	1.439E+02	-2.811E+02	-6.021E+02	-6.971E+02	-6.141E+02	-3.701E+02	-5.072E+00
7.819E+02	9.229E+02	5.919E+02	1.659E+02	-1.307E+01	-2.431E+02	-5.231E+02	-6.931E+02	-6.481E+02	-2.881E+02
4.239E+02	8.609E+02	7.509E+02	3.799E+02	5.928E+00	-3.771E+02	-4.641E+02	-5.711E+02	-4.621E+02	-1.707E+01
3.139E+02	3.049E+02	2.799E+02	1.439E+02	-6.007E+01	-1.931E+02	-1.651E+02	2.949E+02	2.629E+02	8.093E+01
-8.507E+01	-2.021E+02	-1.011E+02	3.379E+02	3.079E+02	7.793E+01	-2.411E+02	-4.541E+02	-4.831E+02	-2.381E+02
2.479E+02	9.499E+02	9.139E+02	5.029E+02	4.993E+01	-3.961E+02	-7.391E+02	-8.381E+02	-7.341E+02	-2.791E+02
6.329E+02	1.009E+03	8.449E+02	4.139E+02	4.193E+01	-3.391E+02	-5.451E+02	-6.081E+02	-5.461E+02	-2.901E+02
-2.907E+01	4.219E+02	5.149E+02	3.809E+02	1.079E+02	-1.981E+02	-3.891E+02	-4.171E+02	-2.911E+02	-2.007E+01
4.219E+02	5.379E+02	2.819E+02	-7.207E+01	-3.611E+02	-4.171E+02	-3.971E+02	-3.007E+01	2.529E+02	2.949E+02
1.869E+02	7.493E+01	-5.507E+01	-2.641E+02	-4.471E+02	-5.171E+02	-3.531E+02	1.679E+02	7.319E+02	7.519E+02
4.239E+02	1.493E+01	-3.531E+02	-5.701E+02	-7.161E+02	-6.281E+02	-2.701E+02	1.579E+02	4.889E+02	7.029E+02
5.569E+02	2.999E+02	5.928E+00	-2.961E+02	-5.381E+02	-6.431E+02	-5.231E+02	-2.301E+02	1.589E+02	4.069E+02
3.989E+02	1.969E+02	2.928E+00	-9.907E+01	-1.881E+02	-3.241E+02	-3.321E+02	-1.181E+02	-1.007E+01	1.093E+01
1.993E+01	8.093E+01	1.029E+02	2.019E+02	3.939E+02	2.079E+02	-1.531E+02	-4.411E+02	-5.311E+02	-1.651E+02
6.769E+02	7.629E+02	5.619E+02	2.079E+02	-2.321E+02	-5.071E+02	-8.391E+02	-8.081E+02	-4.571E+02	2.309E+02
8.779E+02	1.042E+03	8.459E+02	3.359E+02	-1.791E+02	-5.901E+02	-8.521E+02	-9.091E+02	-7.251E+02	-2.871E+02
4.509E+02	8.179E+02	7.509E+02	7.429E+02	4.169E+02	2.928E+00	-2.851E+02	-5.741E+02	-8.051E+02	-7.931E+02
-6.211E+02	-3.031E+02	4.379E+02	1.002E+03	1.032E+03	6.539E+02	5.093E+01	-5.141E+02	-8.701E+02	-9.771E+02
-8.981E+02	-5.191E+02	3.769E+02	1.023E+03	1.022E+03	7.059E+02	1.869E+02	-3.081E+02	-6.631E+02	-8.121E+02
-6.601E+02	-2.921E+02	5.119E+02	8.509E+02	7.299E+02	3.829E+02	1.769E+02	-4.607E+01	-2.931E+02	-5.171E+02
-5.441E+02	-4.731E+02	-1.671E+02	5.309E+02	1.012E+03	8.619E+02	4.349E+02	1.093E+01	-2.651E+02	-5.531E+02
-7.371E+02	-6.941E+02	-4.401E+02	8.293E+01	8.949E+02	1.041E+03	8.429E+02	4.509E+02	1.119E+02	-1.761E+02
-4.651E+02	-7.101E+02	-8.371E+02	-7.331E+02	-3.781E+02	2.829E+02	8.509E+02	9.549E+02	7.439E+02	4.629E+02
1.389E+02	-3.491E+02	-7.681E+02	-9.931E+02	-9.681E+02	-6.051E+02	4.749E+02	9.779E+02	8.639E+02	4.629E+02
2.793E+01	-3.191E+02	-5.221E+02	-5.601E+02	-4.371E+02	-1.691E+02	-4.007E+01	7.693E+01	2.709E+02	1.709E+02
-7.707E+01									

Table 3. Filtered time series of 1 Hz

YAB(M) =

1.755E+00	1.653E+00	1.497E+00	1.311E+00	1.114E+00	9.178E-01	7.144E-01	5.087E-01	2.835E-01	-3.303E-02
-3.733E-01	-7.411E-01	-1.095E+00	-1.405E+00	-1.654E+00	-1.833E+00	-1.947E+00	-2.004E+00	-2.009E+00	-1.969E+00
-1.873E+00	-1.721E+00	-1.527E+00	-1.317E+00	-1.090E+00	-9.138E-01	-5.139E-01	-1.747E-01	2.055E-01	5.277E-01
1.049E+00	1.423E+00	1.721E+00	1.952E+00	2.124E+00	2.271E+00	2.329E+00	2.361E+00	2.359E+00	2.314E+00
2.207E+00	2.039E+00	1.808E+00	1.520E+00	1.182E+00	9.007E-01	3.473E-01	-1.316E-02	-4.030E-01	-7.766E-01
-1.124E+00	-1.452E+00	-1.774E+00	-2.071E+00	-2.314E+00	-2.494E+00	-2.568E+00	-2.544E+00	-2.417E+00	-2.220E+00
-2.003E+00	-1.763E+00	-1.499E+00	-1.195E+00	-8.527E-01	-4.553E-01	-3.425E-02	4.415E-01	9.324E-01	1.364E+00
1.721E+00	2.012E+00	2.244E+00	2.437E+00	2.534E+00	2.669E+00	2.739E+00	2.739E+00	2.653E+00	2.474E+00
2.224E+00	1.918E+00	1.577E+00	1.211E+00	8.294E-01	4.324E-01	3.207E-02	-3.763E-01	-8.152E-01	-1.252E+00
-1.659E+00	-2.016E+00	-2.308E+00	-2.527E+00	-2.665E+00	-2.725E+00	-2.702E+00	-2.620E+00	-2.512E+00	-2.376E+00
-2.188E+00	-1.938E+00	-1.621E+00	-1.252E+00	-8.459E-01	-3.448E-01	9.042E-02	5.551E-01	9.974E-01	1.405E+00
1.767E+00	2.073E+00	2.304E+00	2.477E+00	2.602E+00	2.682E+00	2.714E+00	2.695E+00	2.610E+00	2.456E+00
2.238E+00	1.961E+00	1.622E+00	1.223E+00	7.740E-01	3.064E-01	-1.509E-01	-5.579E-01	-9.069E-01	-1.203E+00
-1.461E+00	-1.689E+00	-1.900E+00	-2.083E+00	-2.239E+00	-2.331E+00	-2.345E+00	-2.282E+00	-2.149E+00	-1.963E+00
-1.674E+00	-1.376E+00	-1.055E+00	-7.359E-01	-4.079E-01	[illegible]	2.142E-01	5.680E-01	7.495E-01	1.079E+00
1.350E+00	1.572E+00	1.737E+00	1.844E+00	1.893E+00	1.491E+00	1.853E+00	1.788E+00	1.700E+00	1.564E+00
1.377E+00	1.148E+00	8.780E-01	5.706E-01	2.559E-01	-3.241E-02	-2.733E-01	-4.551E-01	-6.115E-01	-7.703E-01
-9.374E-01	-1.102E+00	-1.262E+00	-1.392E+00	-1.472E+00	-1.448E+00	-1.434E+00	-1.317E+00	-1.150E+00	-9.641E-01
-7.811E-01	-6.174E-01	-4.840E-01	-3.549E-01	-2.132E-01	-5.052E-02	1.333E-01	3.500E-01	5.576E-01	7.379E-01
8.751E-01	9.585E-01	9.754E-01	9.480E-01	9.010E-01	9.451E-01	7.856E-01	7.267E-01	6.694E-01	5.759E-01
4.833E-01	4.006E-01	3.405E-01	3.107E-01	2.479E-01	2.706E-01	2.097E-01	1.150E-01	4.513E-03	-8.987E-02
-1.644E-01	-2.124E-01	-2.354E-01	-2.371E-01	-2.224E-01	-2.014E-01	-1.314E-01	-1.686E-01	-1.574E-01	-1.495E-01
-1.509E-01	-1.687E-01	-1.717E-01	-1.541E-01	-1.159E-01	-6.615E-02	-2.424E-02	-4.674E-03	-6.459E-03	-2.350E-02
-5.603E-02	-1.058E-01	-1.490E-01	-1.713E-01	-1.670E-01	-1.457E-01	-1.216E-01	-1.069E-01	-1.025E-01	-7.802E-02
-1.008E-01	-1.047E-01	-1.191E-01	-1.235E-01	-1.108E-01	-7.224E-02	-1.343E-02	5.743E-02	4.230E-02	4.565E-02
-2.287E-02	-8.752E-02	-1.217E-01	-1.045E-01	-5.294E-02	3.777E-02	1.406E-01	2.278E-01	2.523E-01	2.233E-01
1.417E-01	6.046E-02	1.835E-03	-2.460E-02	-1.419E-02	3.107E-02	9.949E-02	1.784E-01	2.317E-01	2.159E-01
1.503E-01	6.189E-02	-2.127E-02	-8.022E-02	-1.142E-01	-1.221E-01	-1.011E-01	-6.247E-02	-2.604E-02	-9.292E-03
-1.911E-02	-5.567E-02	-1.096E-01	-1.691E-01	-2.214E-01	-2.611E-01	-2.847E-01	-2.765E-01	-2.253E-01	-1.315E-01
-2.760E-02	4.844E-02	8.280E-02	8.009E-02	3.432E-02	-2.765E-02	-4.005E-02	-1.123E-01	-7.641E-02	2.520E-03

Table 4. Filtered time series of 4 Hz

YAB(M)=

3.791E+01	2.663E+01	5.512E+00	-1.752E+01	-3.393E+01	-3.743E+01	-2.654E+01	-5.563E+00	1.775E+01	3.415E+01
3.732E+01	2.592E+01	4.292E+00	-1.940E+01	-3.592E+01	-3.427E+01	-2.546E+01	-2.492E+00	2.040E+01	3.544E+01
3.829E+01	2.478E+01	1.863E+00	-2.131E+01	-3.557E+01	-3.593E+01	-2.227E+01	-1.473E-01	2.171E+01	3.494E+01
3.417E+01	2.022E+01	-1.232E+00	-2.182E+01	-3.353E+01	-3.219E+01	-1.931E+01	2.491E+00	2.202E+01	3.270E+01
3.044E+01	1.627E+01	-4.115E+00	-2.252E+01	-3.159E+01	-2.405E+01	-1.316E+01	6.754E+00	2.351E+01	3.039E+01
2.485E+01	9.467E+00	-9.489E+00	-2.431E+01	-2.902E+01	-2.195E+01	-6.331E+00	1.149E+01	2.444E+01	2.749E+01
1.982E+01	4.565E+00	-1.194E+01	-2.331E+01	-2.499E+01	-1.441E+01	-1.676E+00	1.360E+01	2.292E+01	2.257E+01
1.279E+01	-2.074E+00	-1.554E+01	-2.205E+01	-1.897E+01	-7.932E+00	6.243E+00	1.740E+01	2.074E+01	1.491E+01
2.461E+00	-1.101E+01	-1.943E+01	-1.694E+01	-9.876E+00	3.845E+00	1.523E+01	2.158E+01	1.758E+01	5.447E+00
-9.796E+00	-2.166E+01	-2.512E+01	-1.770E+01	-1.735E+00	1.635E+01	2.901E+01	3.039E+01	1.914E+01	-3.455E-01
-2.119E+01	-3.434E+01	-3.401E+01	-2.000E+01	2.301E+00	2.416E+01	3.474E+01	3.485E+01	1.424E+01	-3.949E+00
-2.546E+01	-3.694E+01	-3.393E+01	-1.790E+01	4.640E+00	2.480E+01	3.492E+01	3.130E+01	1.575E+01	-3.262E+00
-2.334E+01	-3.159E+01	-2.720E+01	-1.257E+01	5.907E+00	2.063E+01	2.602E+01	2.191E+01	9.430E+00	-3.752E+00
-1.565E+01	-1.838E+01	-1.336E+01	-3.875E+00	5.635E+00	1.127E+01	1.121E+01	6.274E+00	-6.044E-01	-3.742E+00
-6.923E+00	-3.893E+00	1.148E+00	5.217E+00	5.969E+00	2.730E+00	-2.974E+00	-9.296E+00	-1.025E+01	-7.215E+00
1.578E-01	8.766E+00	1.459E+01	1.473E+01	8.474E+00	-2.037E+00	-1.270E+01	-1.497E+01	-1.904E+01	-1.007E+01
2.343E+00	1.459E+01	2.196E+01	2.112E+01	1.249E+01	-1.057E+00	-1.442E+01	-2.271E+01	-2.285E+01	-1.472E+01
-1.258E+00	1.266E+01	2.208E+01	2.374E+01	1.715E+01	4.720E+00	-9.337E+00	-2.036E+01	-2.441E+01	-2.012E+01
-8.730E+00	5.994E+00	1.895E+01	2.543E+01	2.295E+01	1.219E+01	-3.356E+00	-1.425E+01	-2.663E+01	-2.495E+01
-1.362E+01	3.193E+00	1.898E+01	2.753E+01	2.546E+01	1.315E+01	-4.636E+00	-2.168E+01	-2.831E+01	-2.404E+01
-9.420E+00	9.414E+00	2.440E+01	2.899E+01	2.095E+01	3.111E+00	-1.656E+01	-2.931E+01	-2.916E+01	-1.594E+01
4.901E+00	2.455E+01	3.424E+01	2.925E+01	1.079E+01	-1.372E+01	-3.367E+01	-3.994E+01	-2.402E+01	-4.641E+00
2.321E+01	4.274E+01	4.513E+01	2.840E+01	-1.132E+00	-3.167E+01	-5.052E+01	-4.930E+01	-2.771E+01	6.017E+00
3.823E+01	5.571E+01	5.119E+01	2.625E+01	-9.345E+00	-4.172E+01	-5.809E+01	-5.193E+01	-2.549E+01	1.091E+01
4.316E+01	5.862E+01	5.165E+01	2.462E+01	-1.146E+01	-4.279E+01	-5.732E+01	-4.976E+01	-2.345E+01	1.135E+01
4.129E+01	5.500E+01	4.736E+01	2.172E+01	-1.158E+01	-3.953E+01	-5.145E+01	-4.346E+01	-1.948E+01	1.098E+01
3.626E+01	4.711E+01	4.003E+01	1.834E+01	-9.310E+00	-3.235E+01	-4.280E+01	-3.757E+01	-1.885E+01	5.119E+00
2.815E+01	3.939E+01	3.612E+01	1.997E+01	-2.870E+00	-2.433E+01	-3.498E+01	-3.626E+01	-2.241E+01	-5.192E-01
2.144E+01	3.544E+01	3.645E+01	2.423E+01	3.286E+00	-1.866E+01	-3.372E+01	-3.637E+01	-2.565E+01	-3.576E+00
1.645E+01	3.230E+01	3.614E+01	2.656E+01	7.134E+00	-1.500E+01	-3.151E+01	-3.630E+01	-2.740E+01	-3.004E+00

RUN -0CENTRAL FREQUDNCY= 4.000E+00 PERIOD= 2.500E-01 SPECTRUM DENSITY= 1.130E+03

Table 5. Filtered time series of 7 Hz

YAB(M)=

3.072E+00	2.967E+00	5.212E-02	-2.194E+00	-1.719E+00	4.300E-01	2.211E+00	2.665E+00	1.296E+00	-1.579E+00
-4.260E+00	-4.096E+00	-4.943E-02	4.556E+00	5.171E+00	1.266E+00	-3.039E+00	-3.433E+00	-5.434E-01	1.922E+00
1.146E+00	-1.990E+00	-3.030E+00	-5.173E-01	2.938E+00	4.134E+00	2.317E+00	-5.036E-01	-3.470E+00	-3.843E+00
-1.210E+00	2.292E+00	3.299E+00	4.745E-01	-2.882E+00	-3.767E+00	-2.409E-01	4.880E+00	6.143E+00	1.120E+00
-6.161E+00	-8.574E+00	-2.187E+00	7.477E+00	1.001E+01	1.981E+00	-8.332E+00	-9.494E+00	-2.524E-01	8.996E+00
7.692E+00	-2.222E+00	-9.564E+00	-6.207E+00	4.094E+00	1.015E+01	5.923E+00	-4.205E+00	-9.523E+00	-5.135E+00
3.278E+00	7.446E+00	4.002E+00	-2.355E+00	-4.633E+00	-1.112E+00	3.548E+00	3.216E+00	-1.456E+00	-4.777E+00
-3.177E+00	1.647E+00	3.848E+00	1.223E+00	-2.115E+00	-1.224E+00	2.759E+00	2.923E+00	-1.048E+00	-4.486E+00
-3.020E+00	2.201E+00	5.273E+00	2.772E+00	-3.120E+00	-6.369E+00	-3.202E+00	3.208E+00	6.015E+00	2.618E+00
-3.340E+00	-5.057E+00	-6.355E-01	4.787E+00	4.989E+00	-7.836E-01	-5.937E+00	-4.638E+00	1.254E+00	5.154E+00
3.227E+00	-1.866E+00	-4.062E+00	-5.983E-01	4.679E+00	4.896E+00	-1.377E+00	-7.251E+00	-6.065E+00	1.241E+00
7.126E+00	5.340E+00	-1.604E+00	-5.581E+00	-2.289E+00	3.623E+00	4.769E+00	1.387E-01	-4.653E+00	-4.115E+00
8.577E-01	3.995E+00	1.761E+00	-2.487E+00	-2.520E+00	1.486E+00	3.564E+00	4.593E-01	-3.687E+00	-2.854E+00
1.750E+00	4.292E+00	1.447E+00	-3.440E+00	-4.419E+00	-5.568E-04	4.311E+00	3.125E+00	-1.541E+00	-3.672E+00
-1.187E+00	2.120E+00	2.577E+00	4.800E-01	-1.519E+00	-1.571E+00	-6.545E-01	-4.987E-01	-2.789E-01	1.446E+00
3.209E+00	1.920E+00	-2.451E+00	-5.170E+00	-2.082E+00	4.234E+00	6.396E+00	6.904E-01	-7.235E+00	-9.073E+00
5.743E-01	1.028E+01	9.985E+00	-1.191E+00	-1.189E+01	-9.863E+00	2.759E+00	1.196E+01	7.977E+00	-4.409E+00
-1.124E+01	-5.353E+00	5.981E+00	1.001E+01	2.202E+00	-8.148E+00	-8.757E+00	9.566E-01	1.005E+01	8.300E+00
-2.073E+00	-9.397E+00	-6.543E+00	2.139E+00	6.412E+00	2.504E+00	-3.514E+00	-3.927E+00	1.943E+00	5.482E+00
3.629E+00	-4.110E+00	-7.945E+00	-3.663E+00	3.779E+00	6.385E+00	1.829E+00	-4.198E+00	-4.262E+00	1.950E+00
6.522E+00	3.171E+00	-4.631E+00	-8.033E+00	-2.724E+00	5.182E+00	7.001E+00	1.259E+00	-4.906E+00	-4.076E+00
1.149E+00	3.732E+00	8.439E-01	-2.919E+00	-2.043E+00	1.784E+00	3.140E+00	5.086E-01	-2.200E+00	-1.630E+00
6.737E-01	1.546E+00	-4.959E-01	-2.512E+00	-1.396E+00	1.849E+00	3.392E+00	1.508E+00	-1.105E+00	-1.803E+00
-5.037E-01	6.720E-01	-8.107E-02	-2.247E+00	-2.072E+00	8.102E-01	3.138E+00	2.381E+00	9.612E-02	-4.045E-01
3.753E-02	-5.759E-01	-2.552E+00	-3.139E+00	-5.185E-01	2.673E+00	2.918E+00	5.485E-01	-4.891E-01	1.132E+00
1.923E+00	-1.145E+00	-5.743E+00	-4.877E+00	1.852E+00	7.056E+00	4.267E+00	-3.143E+00	-5.518E+00	-3.016E-01
5.477E+00	3.962E+00	-3.641E+00	-7.935E+00	-3.183E+00	5.538E+00	8.275E+00	2.142E+00	-5.446E+00	-5.800E+00
8.061E-01	5.524E+00	2.493E+00	-5.006E+00	-7.797E+00	-1.209E+00	8.094E+00	1.003E+01	1.895E+00	-7.769E+00
-8.659E+00	-9.820E-01	5.772E+00	4.759E+00	-1.650E+00	-5.768E+00	-3.095E+00	3.504E+00	7.580E+00	4.812E+00
-2.811E+00	-8.262E+00	-6.386E+00	1.178E+00	6.888E+00	5.285E+00	-1.673E+00	-6.192E+00	-3.112E+00	4.245E+00

RUN -0CENTRAL FREQUDNCY= 7.000E+00 PERIOD= 1.429E-01 SPECTRUM DENSITY= 2.079E+01

Table 6. Filtered time series of 9 Hz

YAB(M)=

2.618E+00	-1.905E+00	-1.619E+00	1.951E+00	1.275E+00	-3.158E+00	-3.979E+00	1.275E-02	2.862E+00	1.737E+00
3.753E-01	8.780E-01	5.715E-01	-1.598E+00	-1.658E+00	5.964E-01	1.506E-01	-2.681E+00	-1.845E+00	3.423E+00
5.000E+00	-1.660E-02	-4.480E+00	-2.145E+00	2.699E+00	1.445E+00	-3.608E+00	-4.442E+00	1.927E+00	7.034E+00
2.912E+00	-4.369E+00	-4.406E+00	1.568E+00	3.740E+00	-4.169E-01	-5.076E+00	-2.667E+00	3.927E+00	5.522E+00
-1.226E+00	-4.406E+00	9.741E-01	4.958E+00	-1.283E-01	-6.448E+00	-3.405E+00	4.327E+00	4.410E+00	-1.835E+00
-2.446E+00	3.128E+00	3.676E+00	-3.420E+00	-6.454E+00	-1.651E-01	4.933E+00	6.339E-01	-4.634E+00	-7.426E-01
5.598E+00	2.451E+00	-5.363E+00	-4.233E+00	3.445E+00	3.395E+00	-3.691E+00	-4.354E+00	3.348E+00	6.732E+00
8.040E-01	-4.950E+00	-3.585E+00	2.408E+00	3.094E+00	-2.146E+00	-3.759E+00	1.368E+00	4.481E+00	6.607E-01
-3.994E+00	-2.633E+00	2.004E+00	3.185E+00	-8.152E-01	-3.649E+00	-7.471E-01	4.190E+00	3.413E+00	-1.704E+00
-4.653E+00	-4.965E-01	4.087E+00	8.629E-01	-5.700E+00	-3.770E+00	4.743E+00	5.474E+00	-1.017E+00	-3.816E+00
-1.832E+00	3.526E+00	2.015E+00	-3.692E+00	-4.701E+00	1.544E+00	6.373E+00	2.785E+00	-3.231E+00	-2.957E+00
1.129E+00	2.139E+00	-8.471E-01	-3.681E+00	-2.437E+00	2.407E+00	5.424E+00	2.491E+00	-2.889E+00	-3.792E+00
1.331E-01	2.859E+00	-1.709E-01	-4.373E+00	-2.683E+00	3.748E+00	6.090E+00	3.554E-01	-5.193E+00	-2.849E+00
3.539E+00	3.548E+00	-2.723E+00	-4.775E+00	4.469E-01	3.604E+00	1.253E+00	-3.198E-01	-6.454E-01	-7.640E-01
-8.393E-01	1.426E+00	2.539E+00	-5.249E-01	-3.589E+00	-1.634E+00	3.010E+00	3.488E+00	-1.596E+00	-4.522E+00
-2.684E-01	4.623E+00	2.461E+00	-2.850E+00	-2.906E+00	1.787E+00	3.375E+00	-8.890E-01	-4.616E+00	-2.043E+00
2.830E+00	2.678E+00	-1.152E+00	-1.695E+00	1.804E+00	2.619E+00	-4.611E-01	-3.579E+00	-1.310E+00	1.856E+00
7.703E-01	-2.131E+00	-9.398E-01	2.924E+00	3.356E+00	-3.741E-01	-2.724E+00	-9.488E-01	4.336E-01	-6.624E-01
-2.225E+00	-4.713E-01	2.236E+00	1.695E+00	-2.356E-01	-1.780E-01	7.420E-01	-1.710E-01	-1.327E+00	-3.579E-01
-2.406E-01	-5.664E-01	-5.033E-01	1.775E+00	3.581E+00	7.194E-01	-3.945E+00	-2.464E+00	2.804E+00	1.423E+00
-3.847E+00	-3.292E+00	4.039E+00	5.419E+00	-1.196E+00	-5.845E+00	-1.094E+00	5.341E+00	2.154E+00	-5.389E+00
-5.511E+00	4.933E+00	9.272E+00	2.484E-01	-8.391E+00	-4.069E+00	6.736E+00	6.056E+00	-6.421E+00	-1.100E+01
1.458E+00	1.307E+01	6.502E+00	-8.332E+00	-9.635E+00	3.511E+00	1.049E+01	-3.212E-01	-1.317E+01	-7.110E+00
9.913E+00	1.297E+01	-1.383E+00	-1.073E+01	-2.859E+00	8.539E+00	5.744E+00	-7.487E+00	-1.147E+01	5.967E-01
1.167E+01	6.558E+00	-5.248E+00	-6.411E+00	2.799E+00	6.283E+00	-1.335E+00	-4.349E+00	-3.470E+00	3.867E+00
4.777E+00	1.336E+00	4.367E-01	3.937E-01	-8.554E-01	-1.256E+00	-2.945E-01	-3.212E-01	-3.141E+00	-2.252E+00
3.434E+00	6.495E+00	1.743E+00	-4.412E+00	-3.254E+00	2.402E+00	2.765E+00	-2.963E+00	-5.325E+00	-2.914E-01
5.399E+00	4.226E+00	-2.494E+00	-4.324E+00	1.471E+00	5.215E+00	1.836E-01	-6.346E+00	-4.574E+00	3.346E+00
5.081E+00	-7.250E-01	-2.944E+00	1.725E+00	4.299E+00	-3.417E-01	-5.199E+00	-2.571E+00	2.441E+00	1.775E+00
-2.921E+00	-1.602E+00	4.856E+00	5.201E+00	-2.029E+00	-5.271E+00	-1.145E+00	4.482E+00	1.535E+00	-3.662E+00

RUN -0CENTRAL FREQUDNCY= 9.000E+00 PERIOD= 1.111E-01 SPECTRUM DENSITY= 1.24[illegible]E+01

4.2 Spectrum Estimation

The computer program for calculating the spectrum is shown in Appendix 5. This program contains the generation of filter function (Sinc function), filtering process (taking the running mean of the filter function), and variance calculation of the filtered stationary time series. Spectra were obtained for the same data by both the Blackman-Tukey method and the technique of this thesis. Results are shown in Figs. 13 and 14 for case 1 and 2 respectively (cf. Chang (1968)). Results of both methods compare very well. Moreover, errors generated by this technique are smaller than those of the Blackman-Tukey method. A constant frequency ratio for the b and width of the low pass filter is chosen as one third and one fourth of the frequency. The figures show that the errors decrease with the band width.

The frequency spectrum of data II are shown in Fig. 15 for case 1, 2, and 3. Local maxima appear at frequencies close to twice and triple that of the dominant frequency f_m. Three distinct regions at high frequency end of spectra are observed where the resulting slopes in a double logarithmic plot are different, but the average slope is pretty close to -5 (cf. Chang 1968). In all the spectra, only relative values of spectra densities are plotted instead of the true spectrum.

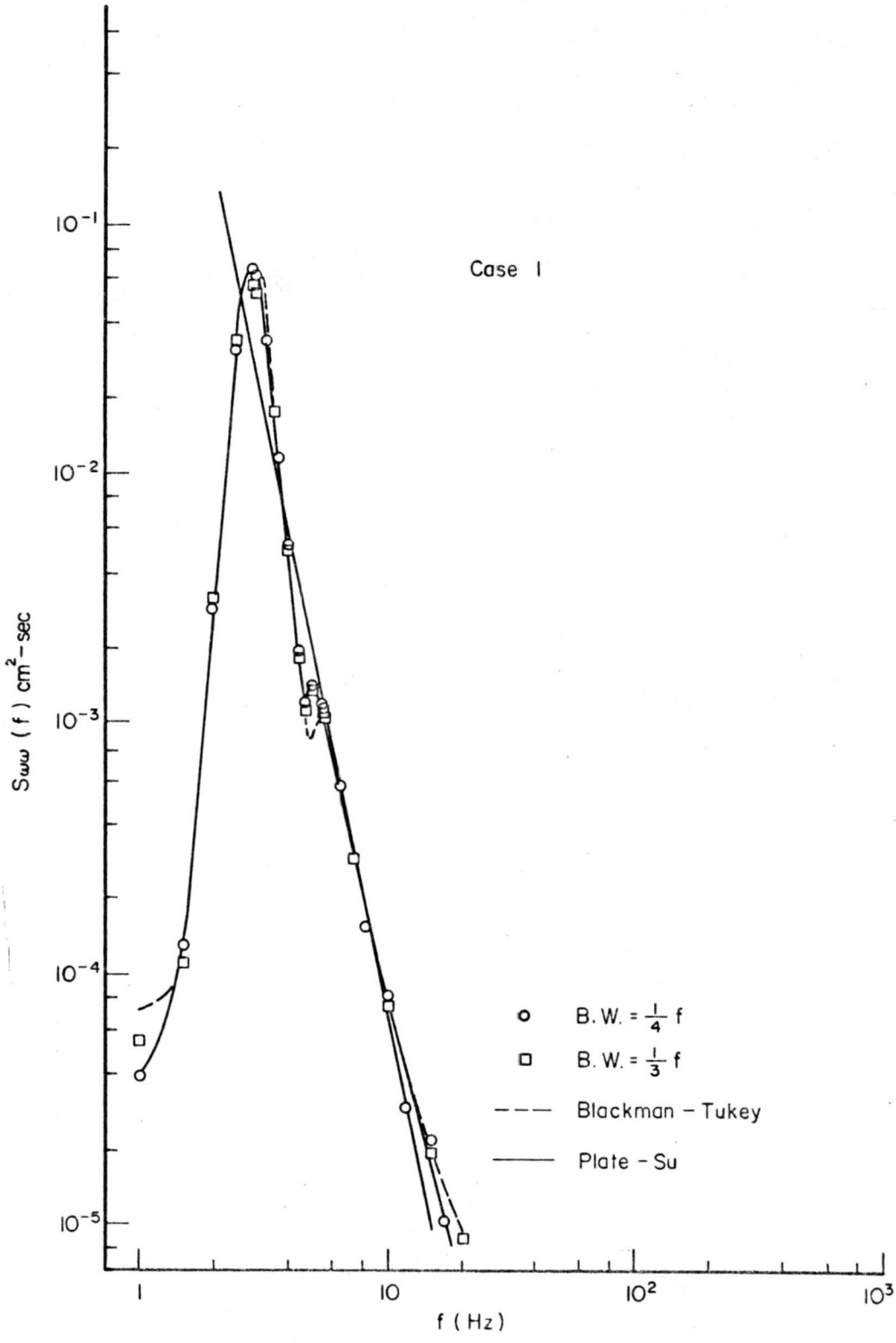

Fig. 13 Spectrum estimation by Blackman-Tukey and Plate-Su technique (Case 1, data I)

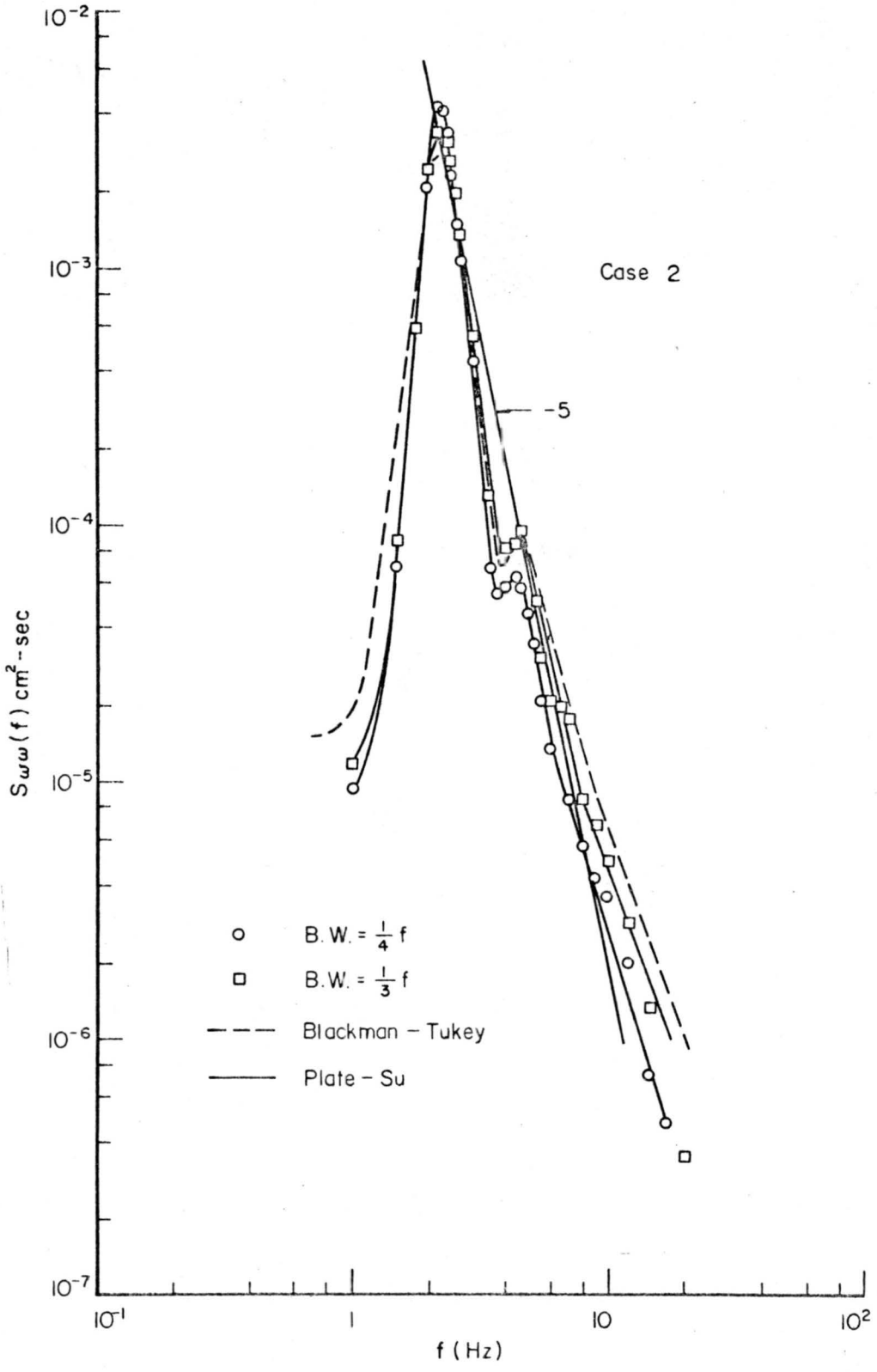

Fig. 14 Spectrum estimation by Blackman-Tukey and Plate-Su technique (Case 2, data I)

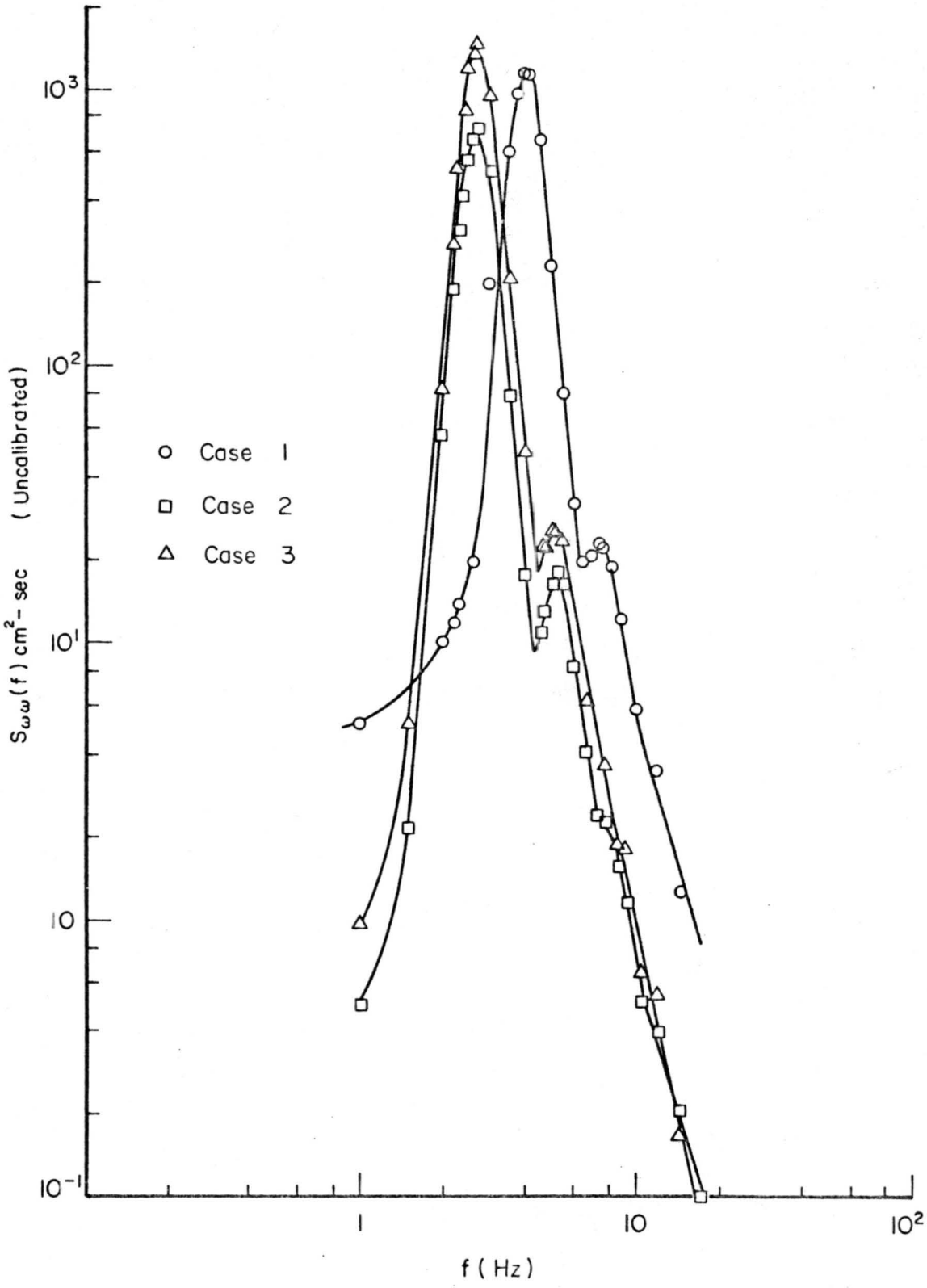

Fig. 15 Spectrum estimation by Plate-Su technique (Case 1, 2, and 3, data II)

4.3 Space-Time Correlation

The original and filtered data at frequency components at frequencies equal to 1, dominant peak frequency f_m, and first local maximum frequency $2 f_m$, were chosen for the auto and space-time correlation analysis. Appendix 6 is the computer program of this analysis, which consists of the generation of filter function, running mean of filter function, calculation of variances of the filtered stationary time series, auto-correlation coefficient and cross-correlation coefficient.

4.3.1 Auto-correlation

The normalized auto-correlation coefficients of data II, case 1 are shown in Fig. 16. It shows that the smaller the filtered frequency component, the longer is the time lag for which data are correlated because the filtered time series at lower frequency components have longer modulated envelopes, as observed in Figs. 10 and 11. The length of these envelopes play a very important role in the correlation. Practically, the correlation is nothing but that of the envelope.

The absolute magnitudes of the auto-correlation curves for the same case are shown in Fig. 18. Of course, the maximum correlation is obtained from the unfiltered time series which contains the total energy, while that of the dominant peak frequency as stated in (4.1) is about 0.7 of the original one.

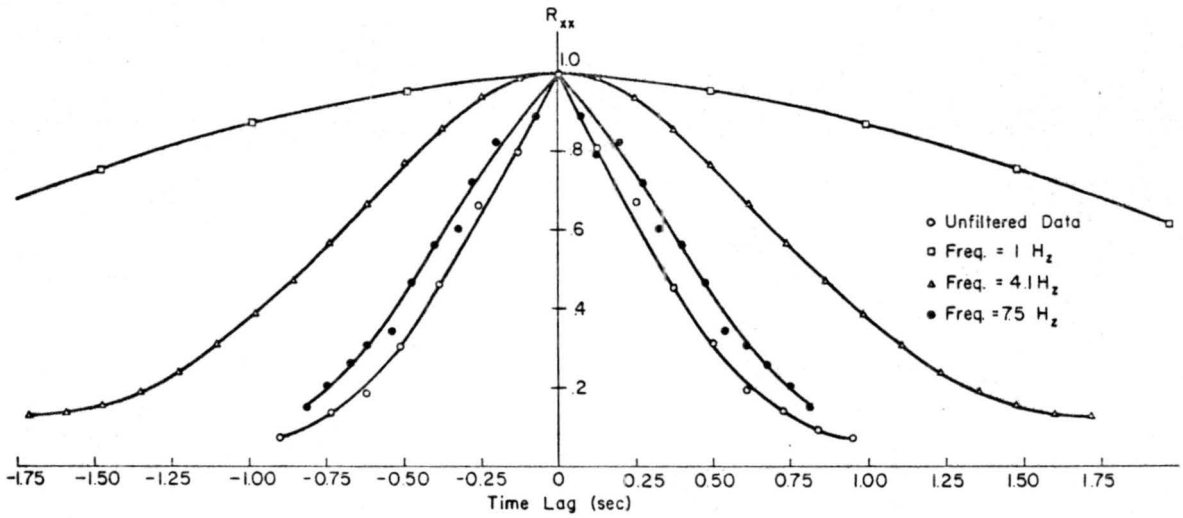

Fig. 16 Normalized auto-correlation coefficient of case 1, data II

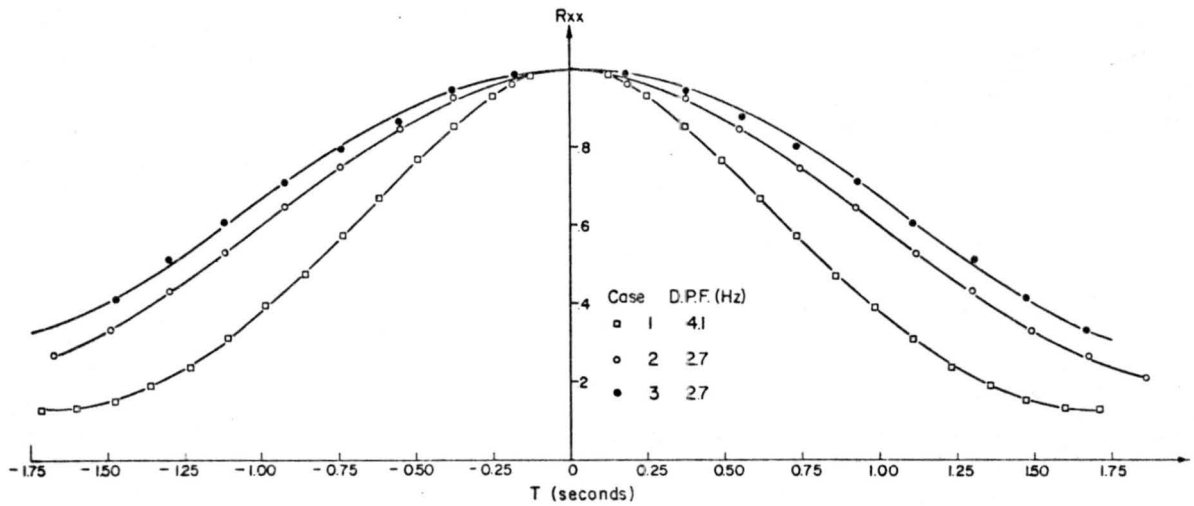

Fig. 17 Relative auto-correlation coefficient of case 1, data II

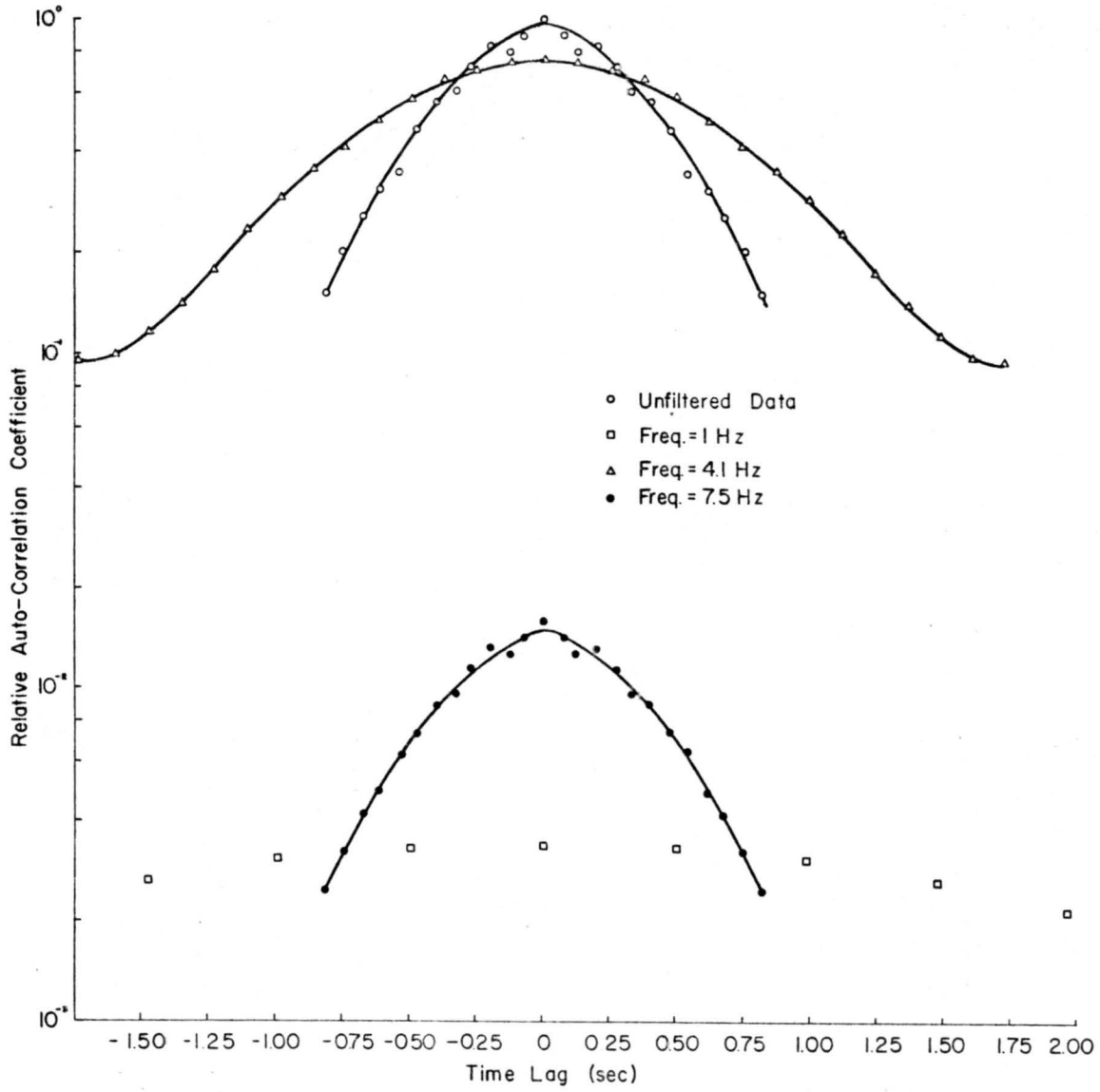

Fig. 18 Auto-correlation of filtered dominant peak

Figure 17 shows the comparison of several cases of auto-correlation coefficients at dominant peak frequency. The characteristics of these curves largely depend on the dominant peak frequency and the fetch. That is, large and long correlation will be obtained for small dominant frequency component and large fetch. Actually, larger fetches have lower dominant frequencies.

4.3.2 Cross-Correlation

Cross-correlation coefficients for the data set II, cases 1, 2, and 3 are shown in Figs. 19 through 21. Figure 19 shows the original data record while the other figures correspond to filtered data at dominant frequency and at the first higher harmonic frequency.

The maximum local maxima of the cross-correlation coefficients occur for the dominant frequency components at 4.1, 2.7, and 2.7 Hz (see Figs. 19, 20, 21). The period between adjacent local maxima of the correlation functions for the filtered data remains constant, and is very close to 1/Freq. This period compares with that of the original data which for most wave groups is equal to the period of the dominant frequency. However, phase shifts are observed between adjacent wave groups, because of the interference of different frequency components. The time lag at which the maximum correlation is observed is found to be 0.12, 0.18, and 0.435 seconds for case 1, 2, and 3 respectively. These optimum time lags remain

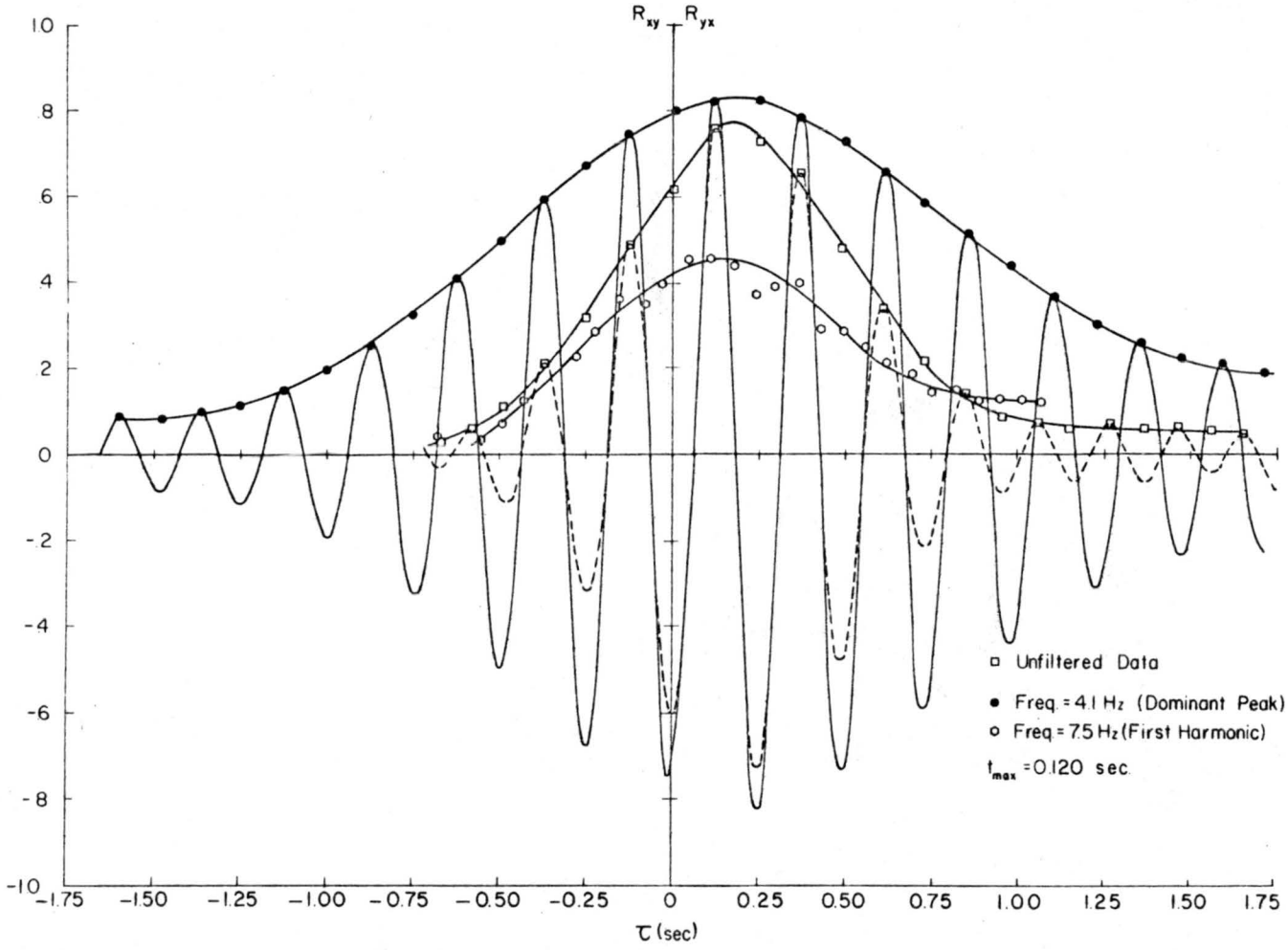

Fig. 19 Cross-correlation of case 1, data II

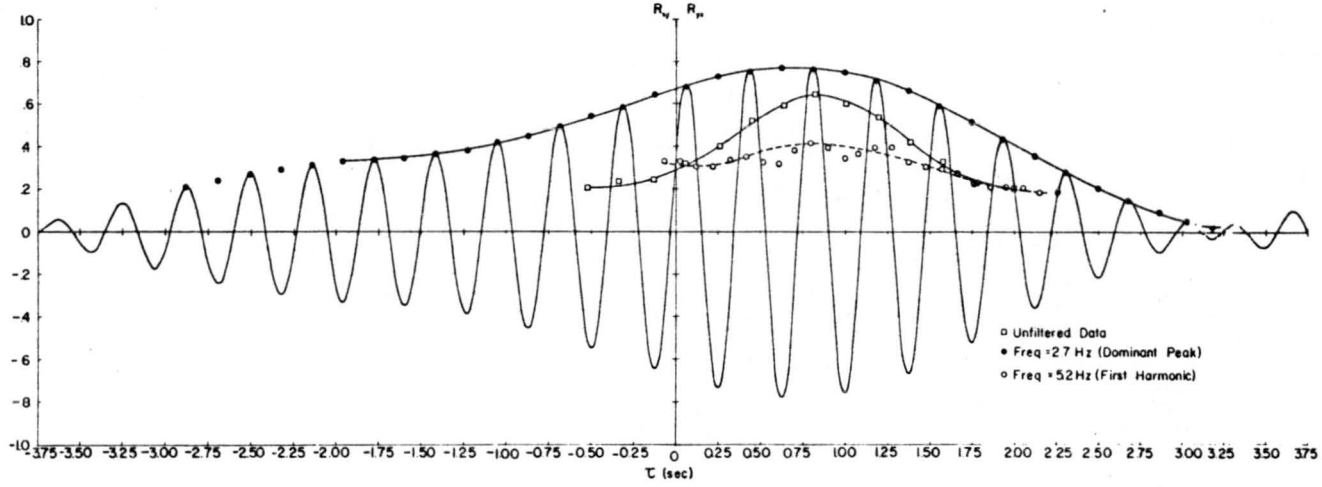

Fig. 20 Cross-correlation of case 2, data II

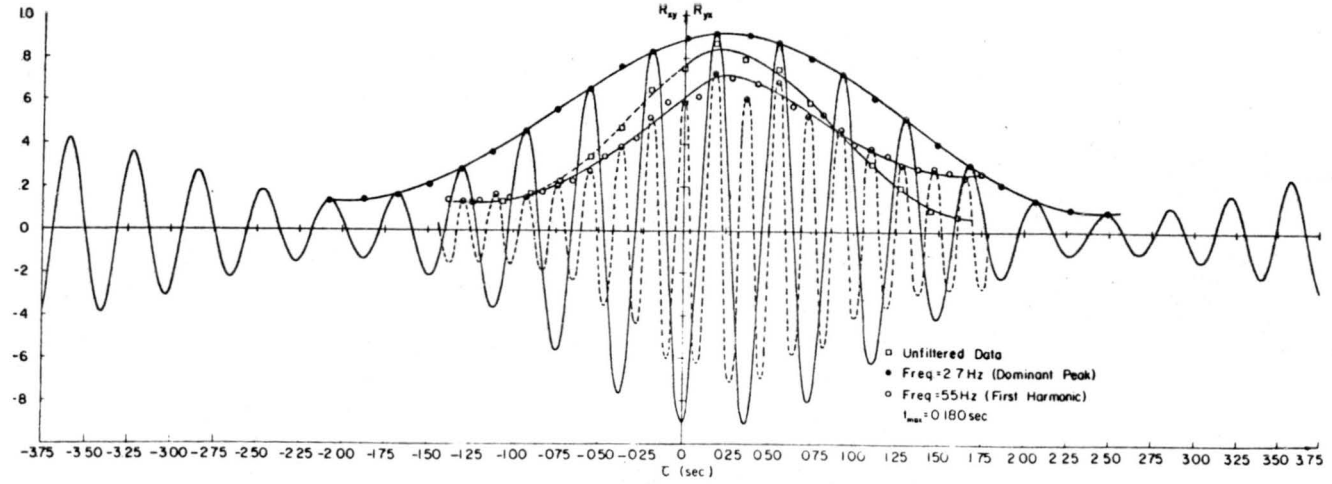

Fig. 21 Cross-correlation of case 3, data II

constant, for all frequency components of a particular case. This means that the time lag for maximum correlation does not depend on the frequency component. In other words, the propagation speed of gravity deep water waves is inversely proportional to the dominant frequency. This is the frequency which must be employed when wave velocities are to be calculated by Eq. (2-17).

In case 3, the time lag for maximum correlation at dominant peak frequency component is 0.435 seconds while that of the original data and local maximum frequency component shifted to 0.825 seconds. This phenomenon is probably caused by the wave decay and growth during its propagation between 2 large distance probes. That is, the wave measured at downstream probe is a different wave than that measured at the upstream probe. The dominant frequencies at the two probes do not differ very much, but for other frequency components the correlations drop rapidly and are quite different. This phenomenon tends to be more pronounced at higher frequency component and larger distances between the two measuring probes.

The following table (4.3.2) is a comparison of phase speed obtained by Eq. 2-20 and Eq. 2-17.

Table 4.3.2

(1) Case	(2) (inch)	(3) c(m/sec) (by Eq. 2-4)	(4) c(m/sec) (by Eq. 2-1)	(5) error (%)	(6) $\bar{c}$(m/sec)	(7) error (%)
1	2.5(6.35cm)	0.508	0.38	32	0.49	4
2	5.2(13.21cm)	0.734	0.57	28.8	0.70	5
3	12(31.5cm)	0.721	0.57	26.5	0.70	3

The values in column (3) are much greater than the theoretical values from Eq. 2-17 (values in column (4)). One reason for the discrepancy lies in neglecting the surface drift velocity u_o in calculating the phase speed. Hidy and Plate (1966) stated, that a comparison should be made only after taking the relative motion of the water into account:

$$\bar{C} = C_o \left\{ 1 + \frac{u_o}{C_o} \left[1 + \frac{3}{2(\bar{k}d)^2} - \frac{1 + 2\cosh(2\bar{k}d)}{\bar{k}d \sinh(2\bar{k}d)} \right] \right\} \qquad (4\text{-}1)$$

where $\bar{k} = 2\pi / \bar{\lambda}$, u_o = water surface velocity, $\bar{\lambda}$ = wave length and $c_o \approx$ square root (g/k). However, if surface tension, finite wave amplitude, and Stokes correction for gravity waves are introduced, then the phase speed will be only 1 to 11% greater than c_o (cf. Hidy and Plate, 1966). Actually, Hidy and Plate (1966) have published experimentally determined wave speeds c for almost identical conditions than those of the present study. If the speeds from their curve are compared with the speeds calculated from the correlations,

then excellent agreement is, indeed, found, as is seen by comparing columns (3) and (6).

4.3.3 Space-Time Correlation

Figures 22 and 23 are the space-time correlation of case 2, 3, and 4 of data II of filtered (at dominant frequency) and original data respectively. Comparison of these two figures shows that for the same distance and time delay, higher correlation was obtained from the filtered data. This phenomena tells that the filtered dominant waves are the most stable, even if compared with the original waves.

4.4 Wave Properties

Results of spectrum calculations show that there are 3 different ranges of energy content and different rates of energy absorption at frequencies larger than the dominant one. The maximum cross correlation versus frequency component curve is shown in Fig. 21. Obviously, the maximum correlation also occurs at dominant peak, 1st local and 2nd local maximum frequency of spectrum estimation.

Growing from the high frequency component, the waves have a constant energy absorption rate, down to the 2nd local maximum frequency, where the energy content and correlation coefficient come to a local maximum. Then the wave decays to a minimum and then grows but with a higher rate of energy absorption until the first local maximum comes. The process will repeat until the dominant peak frequency, where the wave has the maximum energy

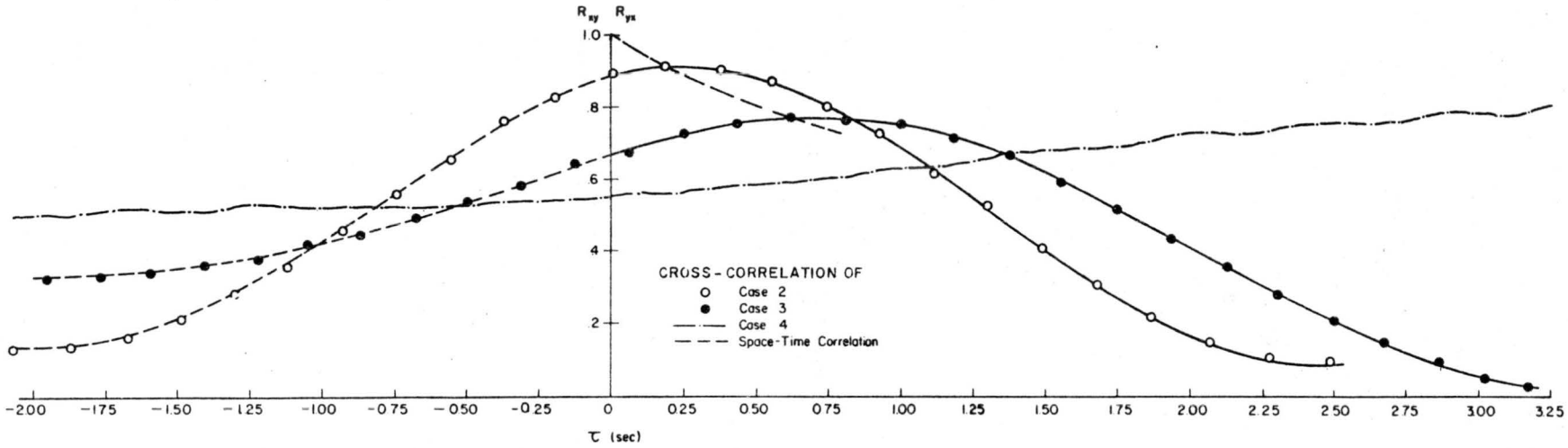

Fig. 22 Space-time correlation of unfiltered time series

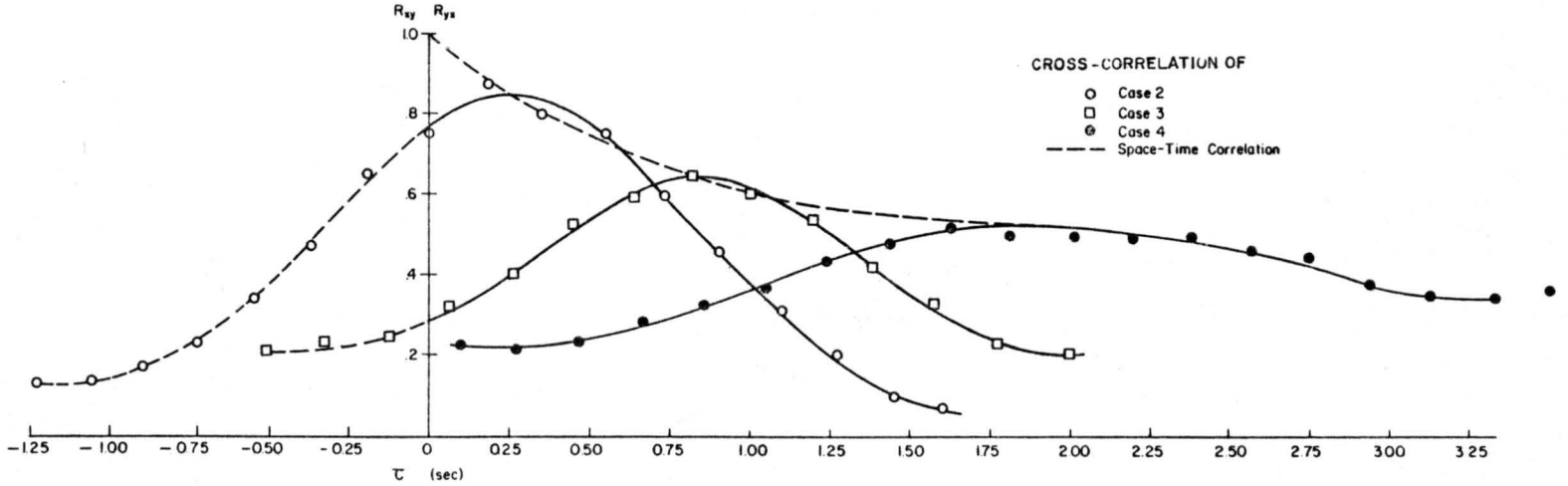

Fig. 23. Space-time correlation of filtered time series at dominant frequency component

content. From the dominant peak down to the zero frequency component, the energy decreases at an almost constant rate (Fig. 24).

Generally, the spectrum and the cross-correlation curves tell about the same properties of gravity, deep water waves.

4.5 Correlations Properties

In each case, if we measure the time lag of a constant percentage of maximum auto-correlation of different frequency components, and plot its reciprocals against bandwidth of the filtered central frequencies, then a linear relation will be obtained. Figure 22 is the typical results of case 1, data II, at 75, 50, and 20% of maximum filtered auto-correlation at central frequencies equal to one, dominant and first local maximum. Practically, larger band width associates with higher frequency component but with lower period in time domain, and so does the shorter length of correlation time lag. So, actually the filtered auto-correlations or cross-correlations do not mean very much but give information about the filter function. As stated in (4.3.1) the properties of the filter function also appear in the filtered time series, which contains larger envelopes of wave groups for smaller band width.

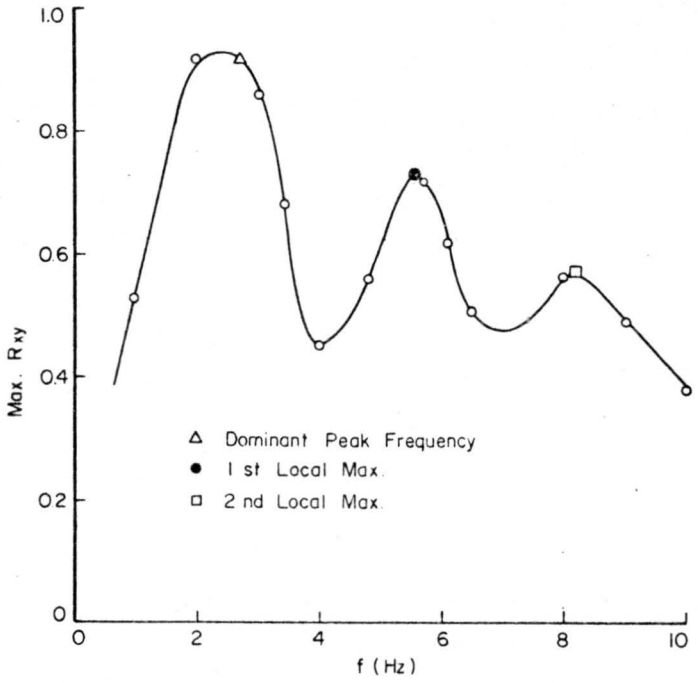

Fig. 24 Maximum cross-correlation of filtered time series

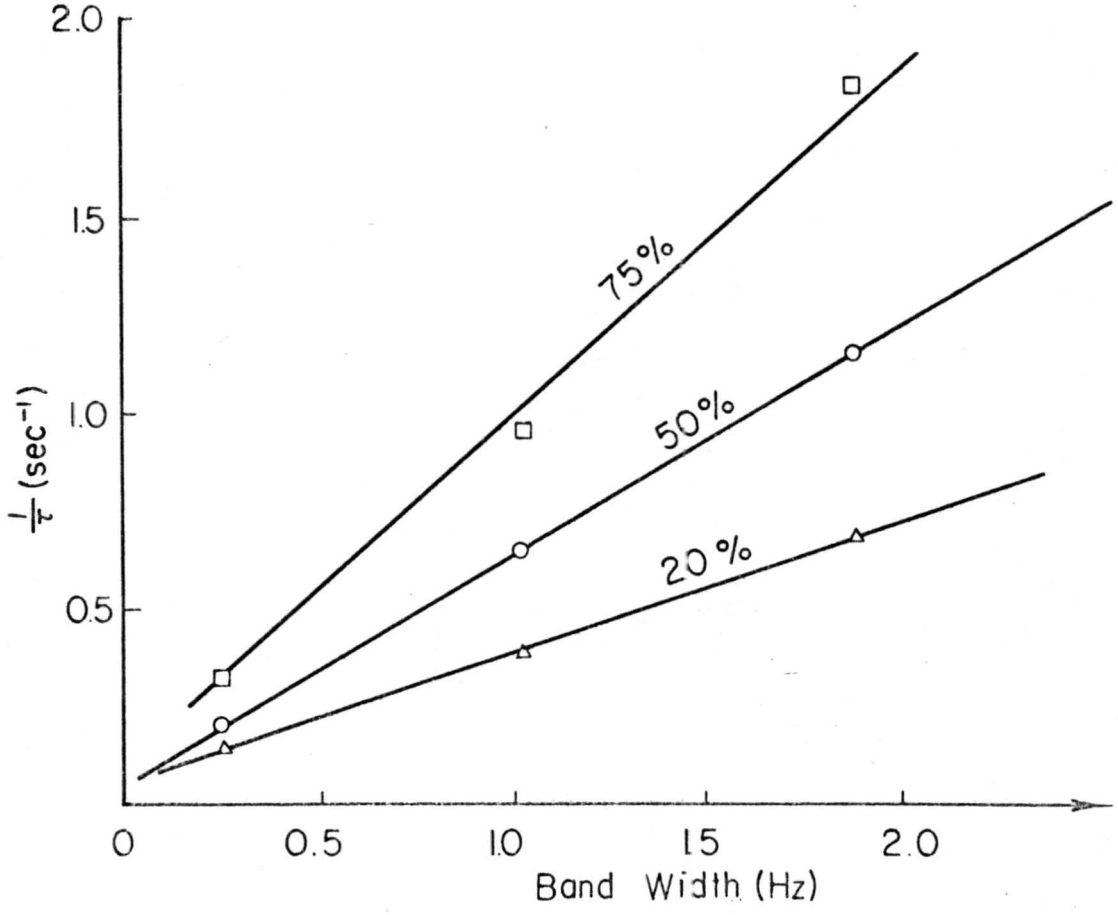

Fig. 25 Linear relations of bandwidth and correlation time lag

Chapter V

CONCLUSIONS AND DISCUSSIONS

5.1 Geometry of the filtered water surface data at dominant frequency component is similar to that of the original data.

5.2 The filter of this study results in a better spectrum estimation than is obtained by many other techniques.

5.3 The auto-correlation curves (Fig. 18) indicates that the filtered data for any of the frequency components show higher correlation than the unfiltered original data.

5.4 The correlation curves are amplitude periodic curves (Fig. 20). The period is inversely proportional to the center frequency of the band pass filter. The maximum amplitude always occurs at maximum correlation, and the wave groups oscillate and then damp out at large t.

5.5 The propagation speed of water waves obtained by this technique is in excellent agreement with experimental results. This technique is therefore a good way for measuring wave speed.

5.6 As far as can be ascertained the filter shape of the band pass filter of this study is better than many other filters. The accuracy of the filter shape can be adjusted by suitably choosing α, which can, according to the desired accuracy be chosen small or large. In this thesis, α has been chosen 8, which gives satisfactory results.

5.7 Suggestions for further study:

5.7.1 For looking into more details of the wave growth and wave decay, further experimental works is needed. It is desired to extend the correlation curves with distance.

5.7.2 Find the error estimation of the digital band pass filter. For this either a digital computer with more digits should be used or a better way of solution of Fourier transform of truncated Sinc function should be worked out.

5.8.3 Shorten the computing time. The computing time for the analysis by the present technique is greater than that required by Blackman-Tukey method. Some improvement of the computer program may be desired which will reduce the computing time greatly.

REFERENCES

Bartlett, M.S. (1948); "Smoothing periodograms from time series with continuous spectra," Nature, Vol. 161, pp. 686-687.

Bartlett, M.S. (1950); "Periodogram analysis and continuous spectra," Biometrika, Vol. 37, pp. 1-16.

Bartlett, M.S. and Mehdi J. (1955); "On the efficiency of procedures of smoothing periodograms from time series with continuous spectra," Biometrika, Vol. 42, pp. 143-150.

Bartlett, M.S. (1963); "The spectral analysis by point process," J. Roy, Stat. Soc., B, Vol. 25, pp. 264-280.

Blackman, R.B. and Tukey, J.W. (1958); "The measurement of power spectra from the point of view of communications of engineering," New York, Dover Publications, Inc., New York.

Bracewell, R.; "The Fourier transform and its application," McGraw-Hill Book Comp., New York.

Brier, G.W. (1961); "Some statistical aspects of long term fluctuations in solar and atmospheric phenomena," Annals, New York Acad. of Sciences, Vol. 95, pp. 173-187.

Carslaw, H.S. (1930); "Introduction to the theory of Fourier series and integrals," MacMillan, New York.

Chang, P.C. (1969); "Laboratory measurement of air flow over wind generated waves," Ph.D. dissertation, Dept. of Civil Engineering, Colorado State University, Fort Collins, Colo.

REFERENCES - CONTINUED

Chuprov, S.D. (1967); "An estimate of the influence of wave dispersion on the spatial correlation of elevations water surface," Atmospheric and Oceanic Physics, Vol. 3, No. 1, pp. 108-110.

Faure, A.J., J.J. Gaviglio, and R. Dumas(1957); "Space-time double correlations and spectra in a turbulent boundary layer," J. of Fluid Mech.

Faure, A.J. (1964); "Review on space-time correlations in turbulent fluids," J. of Applied Mech.

Goodman, N.R. (1961); "Some comments on spectral analysis of time series," Technometrics, Vol. 3, No. 2, pp. 221-228.

Grenander, U. and M. Rosenblatt (1953); "Statistical spectra analysis of time series arising from stationary stochastic process," Annals Math. Stat., Vol. 24, pp.537-558.

Grenander, U. (1958); "Bandwidth and variance in the estimation of spectrum," J. Roy. Stat. Soc., B, Vol. 20, pp. 152-157.

Hidy, G.M. and E.J. Plate (1965); "The frequency spectra of wind generated waves," Physics of fluids, p. 1837.

Hidy, G.M. and E.J. Plate (1966); "Wind action on water standing in a laboratory channel," J. Fluid Mech., Vol. 26, part 4, pp. 651-687.

Holoway, J.L. Jr. (1958); "Smoothing and filtering of time series and space-fields," Advances in Geophysics, Vol 4, pp. 351-389.

Jenkins, G.M. and Priestley, M.B. (1957); "The spectral analysis of time series," J. Roy. Stat. Soc. B, Vol. 19, pp. 1-12.

REFERENCES - CONTINUED

Jenkins, G.M. (1961); "General considerations in the analysis of spectra," Technometrics, Vol. 3, No. 2, pp. 133-166.

Lee, Y.W. (1960); "Statistical theory of communication," John Wiley and Sons, Inc., New York.

Lomnicki, F.A. and Zaremba, S.K. (1959); "Bandwidth and resolvability in statistical spectral analysis," J. Roy. Stat. Soc. B, Vol. 21, pp. 169-171.

Parzan, E. (1957); "On constant estimates of the spectral density of a stationary time series," Ann. Math. Stat., Vol. 28, pp. 329-348.

Parzan, E. (1958); "On asymptotically efficient consistent estimates of the spectral density function of a stationary time series," J. Roy. Stat. Soc. B, Vol. 20, pp. 303-322.

Parzan, E. (1961); "Mathematical considerations in the estimation of spectra," Technometrics, Vol. 3, No. 2, pp. 167-190.

Plate, E.J. and G.M. Hidy (1967); "Laboratory study of air flowing over a smooth surface onto small water waves," Journal of Geophysical Research, Vol. 72, pp. 4627-4641.

Plate, E.J., P.C. Chang, and G.M. Hidy (1968); "Experiments on the generation of smaller water waves by wind," J. of Fluid Mech., to be published.

Plate, E.J., and Nath, J.H. (1968); "Modeling of structures subjected to wind generated waves,"

REFERENCES - CONTINUED

Plate, E.J., "The analysis of experimentally determined stationary time series," Lecture Notes, to be published.

Priestley, M.B. (1962); "Basic considerations in the estimation of spectra," Technometrics, Vol. 4, No. 4, pp. 551-564.

Tukey, J.W. (1959); "An introduction to the measurement of power spectra," Probability and Statistics, edited by U. Grenander, New York: McGraw-Hill, pp. 300-330.

Tukey, J.W. (1961); "Discussing emphasizing the connection between analysis of variance and spectrum analysis," Technometrics, Vol. 3, No. 2, pp. 191-219.

Wiegel, R.L. (1964); "Oceanographical Engineering," Prentice-Hall, Englewood Cliffs.

Wonnacott, T. H. (1961); "Spectral analysis combining a Bartlett window with an associated inner window," Technometrics, Vol. 3, No. 2, pp. 235-243.

APPENDIXES

Appendix 1

Let $F(t) = \operatorname{sinc}(\frac{2t}{T_s}) \sqcap (\frac{t}{T_o})$, then

$$A_{T_s}(\omega) = \int_{-\infty}^{\infty} \operatorname{sinc}(\frac{2t}{T_s}) \sqcap (\frac{t}{T_o})\, e^{-i\omega t}\, dt$$

$$= \int_{-T_o/2}^{T_o/2} \operatorname{sinc}(\frac{2t}{T_s})\, e^{-i\omega t}\, dt$$

$$= \int_{-T_o/2}^{T_o/2} \frac{\sin\pi(2t/T_s)}{\pi(2t/T_s)} [\cos\omega t - i \sin\omega t]dt$$

$$= \int_{-T_o/2}^{T_o/2} \frac{1}{2\pi(2t/T_s)} [\sin(\frac{2\pi t}{T_s} + \omega t) + \sin(\frac{2\pi t}{T_s} - \omega t)]dt$$

$$= \int_{-T_o/2}^{T_o/2} \frac{\sin\pi(2/T_s + \omega/\pi)}{\pi t(2/T_s + \omega/\pi)} [\frac{T_s}{4} (\frac{2}{T_s} + \frac{\omega}{\pi}]dt +$$

$$+ \int_{-T_o/2}^{T_o/2} \frac{\sin\pi t(2/T_s - \omega/\pi)}{\pi t(2/T_s - \omega/\pi)} [\frac{T_s}{4} (\frac{2}{T_s} - \frac{\omega}{\pi})]dt$$

$$= \frac{T_s}{4}(\frac{2}{T_s} + \frac{\omega}{\pi}) \int_{-T_o/2}^{T_o/2} \frac{\sin\pi t(2/T_s + \omega/\pi)}{\pi t(2/T_s + \omega/\pi)} dt +$$

$$+ \frac{T_s}{4} (\frac{2}{T_s} - \frac{\omega}{\pi}) \int_{-T_o/2}^{T_o/2} \frac{\sin\pi t(2/T_s - \omega/\pi)}{\pi t(2/T_s - \omega/\pi)} dt$$

$$= \frac{T_s}{2} (\frac{2}{T_s} + \frac{\omega}{\pi}) \int_{o}^{T_o/2} \frac{\sin\pi t(2/T_s + \omega/\pi)}{\pi t(2/T_s + \omega/\pi)} dt +$$

$$+ \frac{T_s}{2} (\frac{2}{T_s} - \frac{\omega}{\pi}) \int_{-T_o/2}^{T_o/2} \frac{\sin t(2/T_s - \omega/\pi)}{t(2/T_s - \omega/\pi)} dt . \quad (1)$$

Two methods are used in solving this problem:

Method A = By integration

Method B = By numerical integration.

Method A

In equation (1),

$$\text{let} \quad t\left(\frac{2}{T_s} + \frac{\omega}{\pi}\right) = X, \quad \text{then} \quad dt = \frac{dX}{\pi(2/T_s + \omega/\pi)},$$

$$\text{when} \quad t = \frac{T_o}{2}, \qquad X = \frac{\pi T_o}{2}\left(\frac{2}{T_s} + \frac{\omega}{\pi}\right).$$

$$\text{Let} \quad t\left(\frac{2}{T_s} - \frac{\omega}{\pi}\right) = Y, \quad \text{then} \quad dt = \frac{dY}{\pi(2/T_s - \omega/\pi)},$$

$$\text{when} \quad t = \frac{T_o}{2}, \qquad Y = \frac{\pi T_o}{2}\left(\frac{2}{T_s} - \frac{\omega}{\pi}\right).$$

Substitute in Eq. (1):

$$A_{T_s}(\omega) = \frac{T_s}{2}\left(\frac{2}{T_s} + \frac{\omega}{\pi}\right) \int_o^{\frac{\pi T_o}{2}\left(\frac{2}{T_s} + \frac{\omega}{\pi}\right)} \frac{\sin X}{X} \left[\frac{dX}{\pi(2/T_s + \omega/\pi)}\right]$$

$$+ \frac{T_s}{2}\left(\frac{2}{T_s} - \frac{\omega}{\pi}\right) \int_o^{\frac{\pi T_o}{2}\left(\frac{2}{T_s} - \frac{\omega}{\pi}\right)} \frac{\sin Y}{Y} \left[\frac{dY}{\pi(2/T_s - \omega/\pi)}\right]$$

$$= \frac{T_s}{2\pi}\left[\mathrm{Si}\left(\frac{\pi T_o}{T_s} + \frac{\omega T_o}{2}\right) + \mathrm{Si}\left(\frac{\pi T_o}{T_s} - \frac{T_o \omega}{2}\right)\right].$$

Let $T_o/T_s = \alpha$, then

$$A_{T_s}(\omega) = \frac{T_s}{2\pi}\left[\mathrm{Si}\left(\pi\alpha + \frac{\omega\alpha T_s}{2}\right) + \mathrm{Si}\left(\pi\alpha - \frac{\omega\alpha T_s}{2}\right)\right] \qquad (2)$$

Appendix 2

Method B:

In Eq. (1), let $\pi(\frac{2}{T_s} + \frac{\omega}{\pi}) = A$, $\pi(\frac{2}{T_s} - \frac{\omega}{\pi}) = B$, then Eq. (1) becomes:

$$A_{T_s}(\omega) = \frac{T_s}{2\pi}\int_0^{\frac{T_o}{2}} \frac{\sin At}{t}\,dt + \frac{T_s}{2\pi}\int_0^{\frac{T_o}{2}} \frac{\sin Bt}{t}\,dt$$

$$= \frac{T_s}{2\pi}\int_0^{\frac{T_o}{2}} \frac{1}{t}\left[At - \frac{(At)^3}{3!} + \frac{(At)^5}{t!} - \frac{(At)^7}{7!} + \ldots\right]dt$$

$$+ \frac{T_s}{2\pi}\int_0^{\frac{T_o}{2}} \frac{1}{t}\left[Bt - \frac{(Bt)^3}{3!} + \frac{(Bt)^5}{5!} - \frac{(Bt)^7}{7!} + \ldots\right]dt$$

$$= \frac{T_s}{2\pi}\left[\int_0^{\frac{T_o}{2}} \left(A - \frac{A^3t^2}{3!} + \frac{A^5t^4}{5!} - \frac{A^7t^6}{7!} + \ldots\right)dt\right.$$

$$\left. + \int_0^{\frac{T_o}{2}} \left(B - \frac{B^3t^2}{3!} + \frac{B^5t^4}{5!} - \frac{B^7t^6}{7!} + \ldots\right)dt\right]$$

$$= \frac{T_s}{2}\left[A\,\frac{T_o}{2}\left(1 - \frac{(A\frac{T_o}{2})^2}{3\cdot 3!} + \frac{(A\frac{T_o}{2})^4}{5\cdot 5!} - \frac{(A\frac{T_o}{2})^6}{7\cdot 7!} + \ldots\right)\right.$$

$$\left. + B\,\frac{T_o}{2}\left(1 - \frac{(B\frac{T_o}{2})^2}{3\cdot 3!} + \frac{(B\frac{T_o}{2})^4}{5\cdot 5!} - \frac{(B\frac{T_o}{2})^6}{7\cdot 7!} + \ldots\right)\right]$$

$$= \frac{T_s}{2\pi}\left\{\left(\pi\alpha + \frac{\omega\alpha T_s}{2}\right)\left[1 - \frac{(\pi\alpha + \frac{\omega\alpha T_s}{2})^2}{3\cdot 3!} + \frac{(\pi\alpha + \frac{\omega\alpha T_s}{2})^4}{5\cdot 5!}\right.\right.$$

$$\left. - \frac{(\pi\alpha + \frac{\omega\alpha T_s}{2})^6}{7\cdot 7!} + \ldots\right]$$

$$+ \left(\pi\alpha - \frac{\omega\alpha T_s}{2}\right)\left[1 - \frac{(\pi\alpha - \frac{\omega\alpha T_s}{2})^2}{3\cdot 3!} + \frac{(\pi\alpha - \frac{\omega\alpha T_s}{2})^4}{5\cdot 5!}\right.$$

$$\left.\left. - \frac{(\pi\alpha - \frac{\omega\alpha T_s}{2})^6}{7\cdot 7!} + \ldots\right]\right\} .$$

```
 JUNE     *FORTRAN                                                    12/30/68
                PROGRAM SUS
          C     CALCULATION OF SINC FUNCTION
000002          DIMENSION SINC(800)
000002          L=1
000003          FREQ=1.
000005      188 PI=3.141592654
000006          FREQU=FREQ*9./8.
000010          FREQL=FREQ*7./8.
000012          TS=1./FREQ
000013          TSU=1./FREQU
000014          TSL=1./FREQL
000016          TSA=TSL
000016          CHK=8./7.
000020          ALPHA=8.
000022      104 T=0.050
000023          IQ=1
000025      106 XS=2.0*T/TSA
000027          YS=PI*XS
000031          SINC(IQ)=SIN(YS)/YS
000036          IF (XS-ALPHA) 108,110,110
000041      108 T=T+0.050
000043          IQ=IQ+1
000045          GO TO 106
000045      110 J=IQ+2
000047          K=2*IQ+1
000050          KB=K
000051          IA=1
000053      112 SINC(J)=SINC(IA)
000056          IF(J-K) 114,116,116
000060      114 J=J+1
000062          IA=IA+1
000063          GO TO 112
000063      116 JA=1
000064      118 SINC(JA)=SINC(K)
000067          IF (JA-IQ) 120,122,122
000071      120 JA=JA+1
000073          K=K-1
000074          GO TO 118
000074      122 KA=JA+1
000076          SINC(KA)=1.
000100          PRINT 580,(SINC(M),M=1,KB)
000112      580 FORMAT (1H0,5X,*SINC(M)=*/,(5(5X,F14.7)))
000112          IF (L-2) 190,192,192
000115      190 L=L+1
000117          TSA=TSU
000120          GO TO 104
000121      192 CALL EXIT
000122          END
```

```
JUNE      *FORTRAN                                                                   06/27/68
                PROGRAM SU1
          C     CALCULATION OF FOURIER TRANSFORM OF FILTER FUNTIONS
000002          DOUBLE PRECISION A(400),B(400),C(400),GN(400),AREA(2),D(400)
000002          DOUBLE PRECISION CK(400),E(400),F(400),BREA(2),BA1(400),G(400)
000002          DOUBLE PRECISION BA2(400),TS,DELT,ALPHA,DW,A1,A2,F1,F2,PI,CA,AI,W
000002          DOUBLE PRECISION BI,DAREA,TRA,ER,FREQ,ANGV,WTS
000002       42 READ (5,108) FREQ,ALPHA,DW
000014          PI=3.14159265
000016          ANGV=2.0*PI*FREQ
000026          TS=2.0*PI/ANGV
000043          L=1
000044          DELT=TS/6.0
000057        4 PRINT 200
000062          PRINT 100,FREQ,ANGV,TS,DELT,DW,ALPHA
000101          A1 = PI*ALPHA
000107        6 CA=1.0/PI
000122          K = 1
000123          W=0.0
000126        8 A2 = (W*ALPHA*TS)/2.
000151          F1 = (A1 + A2)**2
000163          F2 = (A1 - A2)**2
000175          I = 1
000176          GN(I) = 6.
000201          D(I) = ((-1.)**I)*F1/GN(I)
000223          E(I) = ((-1.)**I)*F2/GN(I)
000253       10 AI=2*(I+1)
000256          BI = AI+1.
000264          D(I+1) = ((-1.)**(I+1))*(ABS(D(I)))*F1/(AI*BI)
000314          E(I+1) = ((-1.)**(I+1))*(ABS(E(I)))*F2/(AI*BI)
000345          F(I) = D(I)/(AI-1.)
000366          G(I) = E(I)/(AI-1.)
000407          IF (ABS(F(I))-1.0D-99) 14,14,12
000421       12 I=I+1
000423          GO TO 10
000423       14 CONTINUE
000423          A(K)=1.0
000426          DO 16 J=1,I
000435       16 A(K) = A(K)+F(J)
000445          BA1(K) = (A1+A2)*A(K)
000462          B(K) = 1.
000464          DO 18 J=1,I
000472       18 B(K) = B(K)+G(J)
000502          BA2(K) = (A1-A2)*B(K)
000517          CK(K) = BA1(K)+BA2(K)
000525          C(K) = CA*CK(K)
000533          BREA(L)=0.
000536          IF (C(K)) 22,24,20
000541       20 K=K+1
000543          W=W+DW
000552          GO TO 8
000552       22 K=K-1
000554          WTS=W-DW
000563          GO TO 26
000563       24 WTS=W
000566       26 PRINT 110,WTS
000573          PRINT 102,(C(I),I=1,K)
000605          IF (K-2*(K/2)) 30,28,30
000610       28 K2=K-3
000612          DO 32 I=1,K2,2
000623       32 BREA(L)=BREA(L)+C(I)+4.0*C(I+1)+C(I+2)
000644          AREA(L)=BREA(L)*DW/3.+DW*(C(K-1)+C(K))/2.0+C(K)*DW/4.0
000731          GO TO 36
000732       30 K2=K-2
000734          DO 34 I=1,K2,2
000745       34 BREA(L)=BREA(L)+C(I)+4.0*C(I+1)+C(I+2)
000766          AREA(L)=BREA(L)*DW/3.0+C(K)*DW/4.0
001026       36 GO TO (38,40),L
001035       38 L=L+1
001037          TS=TS+DELT
001046          GO TO 4
001046       40 DAREA=AREA(1)-AREA(2)
001055          TRA=2.0*PI/TS*(1.0/7.0)
001077          ER=(TRA-DAREA)/TRA*100.0
001124          PRINT 104
001127          PRINT 106,AREA(1),AREA(2),DAREA,TRA,ER
001144          GO TO 42
001145      200 FORMAT (1H0,6X,*FREQ*,11X,*ANGV*,11X,*TS*,13X,*DELT*,11X,*DW*,13X,
               1*ALPHA*)
001145      100 FORMAT (1H0,6(5X,D10.3))
001145      102 FORMAT (1H0,*C(I)=*/,(10(3X,D10.3)))
001145      104 FORMAT (1H0,5X,*AREA(1)*,8X,*AREA(2)*,-X,*DAREA*,10Y,*TRA*,12X,
               1*ER*)
001145      106 FORMAT (1H0,5(5X,D10.3))
001145      108 FORMAT (3(D11.3))
001145      110 FORMAT (1H0,*WTS=*,D10.3)
001145          CALL EXIT
001146          END
```

```
JUNE      *FORTRAN                                                              13/13/63
                PROGRAM P025.4
          C     1.CALCULATION OF WATER WAVES
          C     2.CALCULATION OF SINC FUNCTION
          C     3.FILTERING BY MOVING AVERAGE
          C     4.SPECTRUM ANALYSIS
000002          DIMENSION LX(1500),X(1500),SINC(500),YA(1500),YB(1500),YAB(1500)
000002          DO 800 IJK=1,4
000004          M=1
000005      802 MM=M+13
000007          READ (5,801) NM,(LX(I),I=M,MM),NC
000024      801 FORMAT (14I5)
000024          IF (LX(MM).LT.0) 803,804
000031      803 MM=MM-14
000033          GO TO 820
000033      804 M=M+1
000035          GO TO 802
000035      820 DO 821 IP=1,MM
000044      821 X(IP)=LX(IP)
000045          TX=0.
000047          DO 830 IP=1,MM
000053      830 TX=TX+X(IP)
000056          AM=MM
000057          ATX=TX/AM
000061          DO 831 IP=1,MM
000066      831 X(IP)=X(IP)-ATX
000070      104 READ 302,FREQ
000075      302 FORMAT (F10.3)
000075          IF (FREQ.LT.0) GO TO 800
000076          L=1
000077          PI=3.141592654
000100          FREQU=FREQ*9./8.
000102          FREQL=FREQ*7./8.
000103          TS=1.0/FREQ
000105          TSU=1.0/FREQU
000106          TSL=1.0/FREQL
000107          TSA=TSL
000110          CHK=8./7.
000111          ALPHA=8.
000113      106 T=0.025
000114          IQ=1
000116      106 XS=2.0*T/TSA
000120          YS=PI*XS
000122          SINC(IQ)=SIN(YS)/YS
000127          IF (XS-ALPHA) 108,110,110
000132      108 T=T+0.025
000134          IQ=IQ+1
000136          GO TO 106
000136      110 J=IQ+2
000140          K=2*IQ+1
000141          KB=K
000142          IA=1
000144      112 SINC(J)=SINC(IA)
000147          IF (J-K) 114,116,116
000151      114 J=J+1
000153          IA=IA+1
000154          GO TO 112
000154      116 JA=1
000155      118 SINC(JA)=SINC(K)
000160          IF (JA-IQ) 120,122,122
000162      120 JA=JA+1
000164          K=K-1
000165          GO TO 118
000165      122 KA=JA+1
000167          SINC(KA)=1.0
000171          IF (TSA-CHK) 126,124,126
000173      124 IP=KA
000174          IB=MM-IP+1
000176          IA=2*(IP-1)+1
000200          IC=MM-IA+1
000201          AIC=IC
000203          MIU=MM-100
000205      126 MIP=IP-KA
000207          M=0
000207          JB=1
000210          AKB=KB
000212          IF (L.EQ.1) 128,134
000217      128 YA(JB)=0.
000221          DO 130 LA=1,KB
000232          LAM=LA+M+MIP
000233      130 YA(JB)=YA(JB)+X(LAM)*SINC(LA)
000237          YA(JB)=YA(JB)/AKB
000242          IF (JB.EQ.IC) 160,132
000245      132 JB=JB+1
000250          M=M+1
000251          GO TO 128
000251      160 TSA=TSU
000252          L=L+1
000254          GO TO 106
000255      134 YB(JB)=0.
000257          DO 135 LA=1,KB
000271          LAM=LA+M+MIP
000271      135 YB(JB)=YB(JB)+X(LAM)*SINC(LA)
000275          YB(JB)=YB(JB)/AKB
000300          IF (JB.EQ.IC) 138,140
000304      140 JB=JB+1
000306          M=M+1
000307          GO TO 134
000307      138 DO 142 M=1,IC
000315      142 YAB(M)=YB(M)-YA(M)
000317          YS=0.
000323          DO 144 M=1,IC
000325      144 YS=YS+YAB(M)
000330          YS=YS/AIC
000331          VAR=0.
000332          DO 146 M=1,IC
000340      146 VAR=VAR+(YAB(M)-YS)**2
000343          SD=VAR*9./(AIC*FREQ)
000346          PRINT 148,NO,FREQ,TS,SD
000361      148 FORMAT (1H0,5X,*RUN*,2X,I5,5X,*CENTRAL FREQUENCY=*,F10.3,5X,*PERIO
               1D=*,F10.3,5X,*SPECTRUM DENSITY=*,F10.3)
000361      150 GO TO 104
000362      800 CONTINUE
000364        4 CALL EXIT
000365          END
```